8-1-1992

Electronic properties of sensitizer centers

Dan Zhang

Electronic Properties of Sensitizer Centers

By

Dan Zhang

B. S. East China Institute of Chemical Technology

(1980)

A thesis submitted in partial fulfillment of
the requirements for the degree of Master of Science
in the Center for Imaging Science in the
College of Imaging Arts and Sciences at the
Rochester Institute of Technology

August 1992

Signature of the Author_____

Accepted by Dana G. Marsh Aug. 28, 1992

Coordinator, M. S. Degree Program

Center for Imaging Science
College of Imaging Arts and Sciences
Rochester Institute of Technology
Rochester, New York

CERTIFICATE OF APPROVAL
M. S. DEGREE THESIS

The M. S. degree thesis of Dan Zhang
has been examined and approved by the thesis
committee as satisfactory for the thesis requirement
for the Master of Science degree

Prof. Richard K. Hailstone, Thesis Advisor

Dr. Dana G. Marsh

Dr. Judith M. Harbison

August 28, 1992
Date

THESIS RELEASE PERMISSION FORM

Rochester Institute of Technology

College of Imaging Arts and Sciences

Title of Thesis: **Electronic Properties of Sensitizer Centers**

I, Dan Zhang, hereby grant permission to the Wallace Memorial Library of R.I.T. to reproduce my thesis in whole or in part. Any reproduction will not be for commercial use or profit.

Signature:_____

Date:_____Aug. 28, 1992_____

ELECTRONIC PROPERTIES OF SENSITIZER CENTERS

By

Dan Zhang

Submitted to the Center for Imaging Science
in partial fulfillment of the requirements
for the Master of Science Degree
at the Rochester Institute of Technology

ABSTRACT

This investigation expands on previous photographic studies of the sensitivity of sulfur and sulfur-plus-gold sensitized octahedral AgBr emulsions to long wavelength light. The experimental atmosphere was controlled by a variable temperature vacuum sensitometer which reduced the oxygen and moisture content of emulsion coatings and thereby improved the efficiency of long wavelength sensitivity. The relative sensitivity at long wavelengths was determined as a function of wavelength, sensitizer level, and sensitizer type. The activation energy actually measures the energy for a hole release from an excited sensitizer center and not for an electron release as earlier work has claimed. By correlating the desensitization by O_2 with the measured energy levels, a thermal trap depth of electrons trapped at sensitizer centers was derived.

ACKNOWLEDGEMENTS

The author wishes to extend great appreciation to Professor Richard K. Hailstone, her thesis advisor. This effort may have never been completed without his suggestion of the original topic, his valuable knowledge, guidance, and support.

The author is deeply grateful to Dr. Dana G. Marsh, for his guidance, patience and encouragement during the author's study at R.I.T and valuable advice and comments.

Special thanks are owed to Dr. Judith M. Harbison, for her valuable comments and suggestions for the thesis; to the Eastman Kodak Company for their generous support both of funds and equipment; to the Kodak Research Laboratories for providing the emulsion coatings.

DEDICATION

This thesis is dedicated to my parents, who have endeavored in the photographic industry for eight decades between them, and to my very special friend Jingwei Shi.

TABLE OF CONTENTS

LIST OF TABLES

LIST OF FIGURES

Figure 16. The temperature dependence of long wavelength sensitivity from 25°C to -30°C.

Figure. 17. Environmental desensitization vs activation energy.

Figure 18. A proposed model of energy levels of sulfur sensitizer centers.

Figure. 19. Environmental desensitization vs the energy gap between the lowest vacant level and the conduction band.

I. INTRODUCTION

Chemical sensitization of silver halide emulsions with sulfur or sulfur-plus-gold is a necessary requirement for many practical photographic systems. Through chemical sensitization we produce what we call "sensitizer centers' which improve the efficiency of latent-image formation.[1] Just how these sensitizer centers improve the efficiency remains controversial.[2,3] Much of the debate centers around the electronic properties of these centers. Unfortunately, we have little knowledge of the composition, concentration, or energy levels of those centers critical for improved efficiency. Obviously, this situation presents a major impediment to designing emulsions with higher efficiencies. Improvements in computer modeling of latent-image formation will also require a more detailed understanding of sensitizer centers.[4] In this thesis we begin to address this critical need.

Mott and Gurney[2] suggested that the sulfur sensitizer centers were electron trapping and could concentrate the photoelectrons at latent image sites. The lowest vacant levels of sulfur sensitizer centers were therefore below the conduction band of silver halide. On the other hand, Mitchell[3] proposed that the principal function of silver sulfide in photographic sensitivity is to provide more numerous traps for positive holes than that of the latent sub-image specks and to prevent these specks from regression. According to Mitchell, the lowest vacant electronic levels of the sulfur sensitizer centers were above the conduction band and the important energy

levels were the highest filled levels, which are within the bandgap of the silver halide and increase photographic sensitivity by acting as hole trapping centers.

Hamilton[5] hypothesized that although silver sulfide does not have the proper electron affinity to introduce a new impurity level in the bandgap, the presence of an aggregate of silver sulfide molecules at a positive defect site could either modify the primary relaxation process or provide an additional relaxation mode which would cause a modest increase in the trap depth.

Sulfur sensitization increases the silver halide emulsion intrinsic speed as well as extending its sensitivity to light of longer wavelength (>500 nm).[1] The increase in speed in the intrinsic and the long wavelength region is similar, although the absolute sensitivity is several orders-of-magnitude lower at long wavelength. This difference is presumably primarily due to the large difference in effective absorption coefficient in the two spectral regions.

Recent research by Hamilton, Harbison, and Jeanmaire on the energy levels of sulfur sensitization[6] shows that the long wavelength sensitivity induced by sulfur sensitization and sulfur-plus-gold sensitization increases with increasing exposure temperature. The activation energy calculated from their temperature dependence studies was 0.33 eV for the sulfur sensitized samples and 0.19 eV for the sulfur-plus-gold sensitized samples.

These values were assigned to the thermal depths of electrons trapped at the respective sensitizer centers. Hamilton and coworkers concluded that their temperature dependence results are consistent with the Mott-and-Gurney hypothesis, which asserts that the lowest vacant levels of the sulfur sensitizer centers are below the conduction band and that the driving force for an electron transfer to the conduction band is thermal energy. Moreover, Kellogg and Hodes[7] used a thermally-stimulated current technique to measure the electron trap depth of sulfur and sulfur-plus-gold sensitizer centers, and the values obtained with that method provide further support for the Mott-and-Gurney hypothesis.

The temperature dependence studies of Hamilton *et. al.* raise several concerns. First, the level of the sulfur sensitization used (25 mg S/mole Ag) is about an order of magnitude greater than the optimum sensitization for their emulsion. Hence, the thermal energy data obtained may not be relevant to the optimum sensitization condition. Second, in their temperature dependence studies, the experimental atmosphere was maintained at 50% relative humidity before and during exposure. Any electron loss to oxygen and moisture may cause desensitization and this may affect the temperature dependence. Third, only one wavelength cutoff filter, which blocked light less than 620 nm, was used in their experiment. How the temperature influences the sensitivity in different wavelength ranges is not known. Finally, their experiment involved a relatively long time exposure of 3 to 30 minutes. Low intensity reciprocity failure (LIRF) may affect the experimental results.

For further investigating the location of energy levels of sensitizer centers associated with the energy bands of AgX, and verifying whether the temperature dependence of long wavelength sensitivity of sulfur and sulfur-plus-gold sensitization corresponds to the thermal trap depth of sensitizer centers, we have also used temperature dependence studies to focus on the electronic properties of sensitizer centers. However, our experimental design features certain advantages over those of Hamilton and coworkers. Since a range of sensitization levels, including the optimum, was used, the measured activation energies should bear greater photographic relevance to the energy levels of sensitizer centers. The experimental atmosphere was controlled by a variable temperature vacuum sensitometer which reduced the oxygen and moisture content of the emulsion coatings and thereby improved the efficiency of long wavelength sensitivity. Since we used narrow band filters, the influence of temperature at different wavelengths could be discerned.

In the next section we give the details of our experimental procedures. Then we present the experimental results showing the improved long wavelength sensitivity in vacuum, its intensity dependence, its spectral dependence, and its temperature dependence. In the discussion section we will show that the activation energy for long wavelength sensitivity actually measures the energy for hole release from an excited sensitizer center and not for electron release as earlier work has claimed. Furthermore, by

correlating the desensitization by O_2 with the measured energy levels, we derive the thermal trap depth of electrons trapped at sensitizer centers. These measurements are made as a function of wavelength and sensitizer level. As a result, this work significantly extends our knowledge of the electronic properties of sensitizer centers.

II. EXPERIMENTAL PROCEDURE

2.1. Emulsion and Coatings. AgBr octahedral emulsions (0.5 μm edge length) were finished for 40 minutes at 70°C with four levels of $Na_2S_2O_3 \cdot 5H_2O$ for sulfur sensitization and two levels of $Na_2S_2O_3 \cdot 5H_2O$ plus $KAuCl_4$ for sulfur-plus-gold sensitization (Table. 1). The coatings contained 1 g Ag and 2 g gelatin per square meter.

2.2. Sensitometry. The temperature dependence studies utilized a variable temperature vacuum sensitometer,[8] which provided a wide range of accurate temperature variation and a vacuum outgassing system. The variable temperature vacuum sensitometer consists of four parts — the sample holder, the cryostat, the vacuum system and the light source.

Sample holder: The sample holder allows sequential exposure of twelve 3-inch lengths of 16-mm film. The short film lengths avoid temperature gradients and provide for higher exposure intensities.

Table 1. Levels of Finishing Agents Used in Chemical Sensitization

$NaS_2O_3 \cdot 5H_2O$ mg/silver mole	$KAuCl_4$ mg/silver mole	Code in text
2		2S
4		4S
7		7S
15		15S
2	2	2SA
7	7	7SA

Cryostat: The cryostat is in essence two concentric cylinders creating a stainless steel vacuum jacket. This vacuum jacket is lined with many layers of aluminum-coated Mylar film, which acts as a heat radiation barrier. The sample holder is inserted into the inner cylinder. Temperature variation is achieved with a helium exchange gas that has been externally cooled by flowing it through liquid nitrogen. The cooled exchange gas is then heated to the desired temperature by flowing it over ten 250W disk heaters stacked in the bottom of the inner cylinder. Temperature regulation is achieved by controlling the duty cycle of the heaters in proportion to the deviation from the setpoint. The range of exposure temperatures is

-170°C to 100°C, with temperature control generally ±1°C or better.

Vacuum system: The vacuum system consists of an Edwards direct drive mechanical pump. Ultimate vacuum is $3x10^{-2}$ torr. Samples were typically outgassed for 16 hours, after which the system was returned to room pressure with a flow of helium.

Light source: Exposures are made with a 1000-W tungsten-halogen lamp 63 cm from the film plane. The lamp is run at 7 amp AC with a regulated power supply, and is equipped with an electronic shutter and a filter holder.

2.3. Exposure and Processing. Wavelength selection was accomplished with interference filters. The absorption spectra of the six narrow band filters utilized are shown in Figure 1. For each level of sulfur or sulfur-plus-gold sensitized samples, all six narrow band filters were used, and temperature was varied from room temperature to -30°C. Processing was 6 min in Kodak D-19 developer at 20°C with nitrogen burst agitation.

For LIRF investigation, the experiment was conducted at room temperature with blue, 550 nm and 600 nm cutoff filters, whose absorption spectra are shown in Figure 2. Processing was 40 min in EAA-1 developer at 20°C with nitrogen burst agitation.

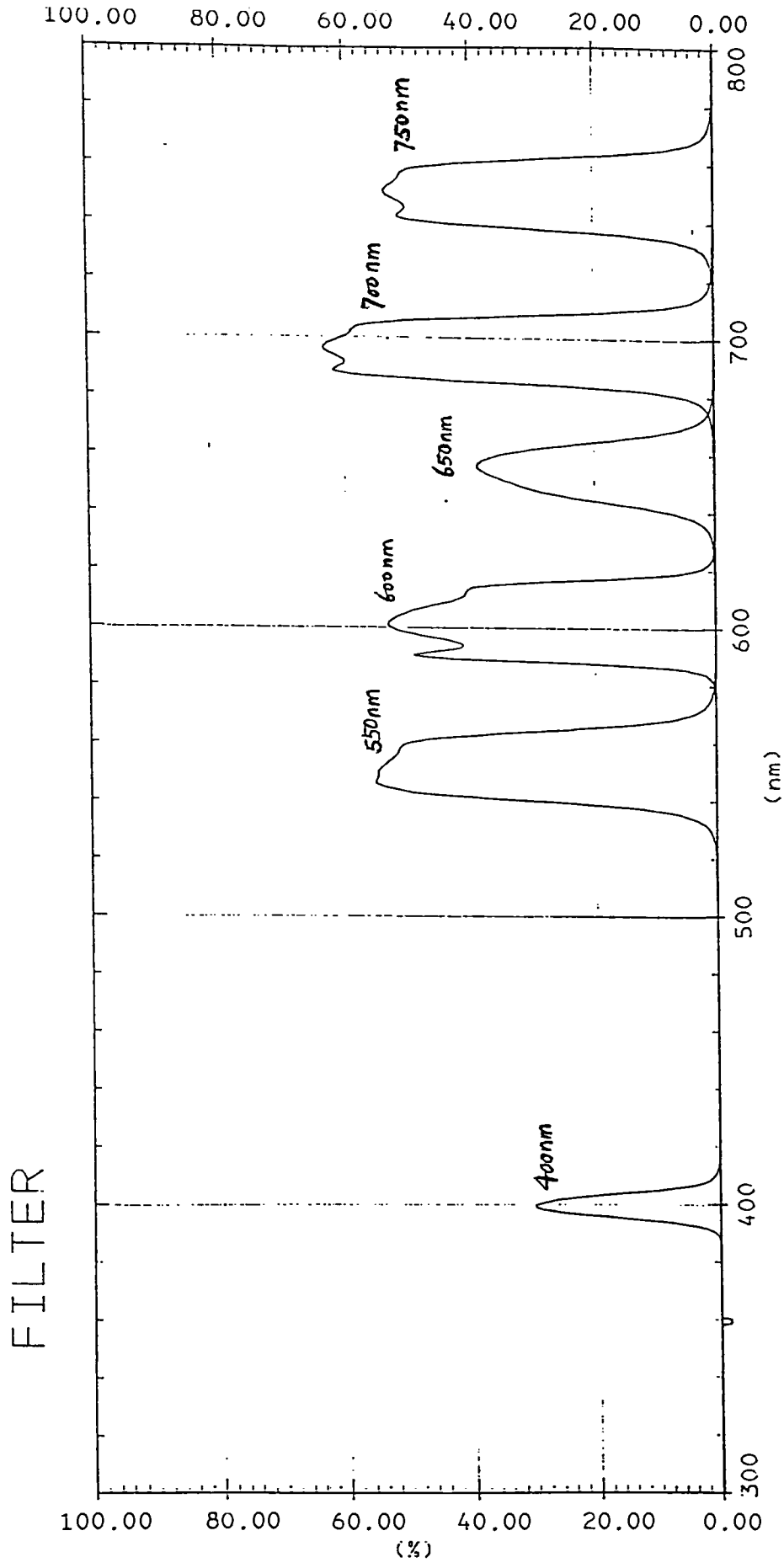

Figure 1. Narrow band filter absorption spectra.

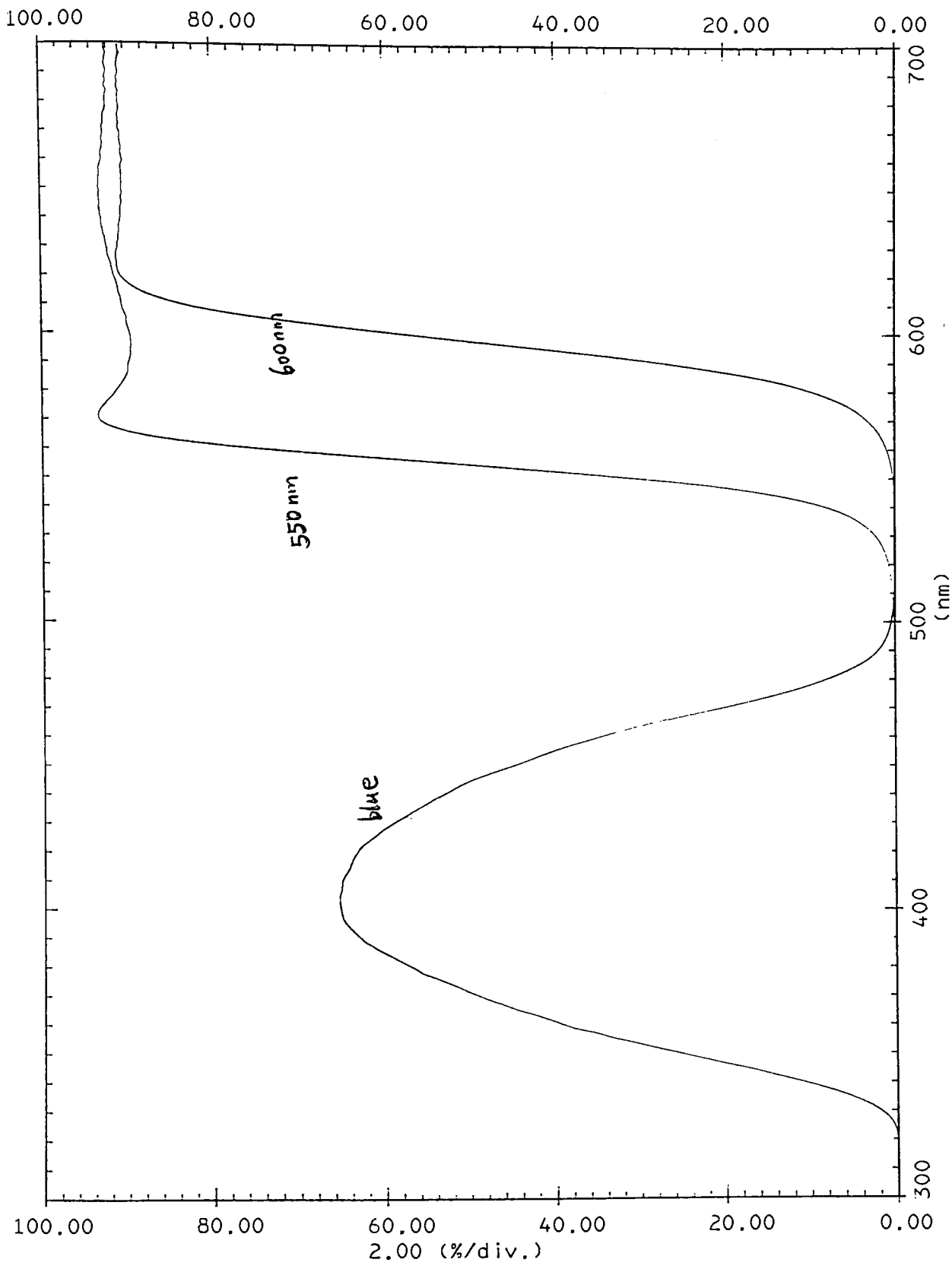

Figure 2. Cutoff filter absorption spectra.

2.4. Speed and Activation Energy Evaluation. Speed is calculated at $D_{ref} = D_{min} + 0.15$. Activation energies are obtained from Arrhenius plots in which speed expressed as LogE is plotted against 1/T. That is, the following relationship is assumed valid

$$E(T) = A \exp(\Delta E/kT) \quad (1)$$

where E(T) is the exposure at temperature T required to produce a fixed density above fog, A is a pre-exponential factor, ΔE is the apparent activation energy, and k is Boltzmann's constant. The ΔE values were obtained from a linear regression fit of the data which also provided a standard deviation of the fit. Tabulated ΔE values include the 2-sigma uncertainties from this regression fit.

III. RESULTS

3.1. Environmental Desensitization. To study the effect of environmental desensitization on the long wavelength sensitivity, samples are exposed with narrow band filters in a vacuum at room temperature and then compared with samples exposed at room pressure and temperature. The D-LogE curves of the 2S and 15S samples exposed at 550 nm, 650 nm and 750 nm are plotted in Figures 3A and 3B, respectively. These data show that vacuum outgassing has only a small effect on samples exposed at 550 nm, but has a significant sensitization effect on samples exposed at 650 nm and 750 nm. The 2S sample showed no detectable speed at 750 nm under room air exposure condition. For these measurements

exposure times were 64 seconds, 256 seconds and 512 seconds for a 550 nm, 650 nm and 750 nm narrow band filter, respectively.

Table 2 summarizes the effect of environmental desensitization on long wavelength exposure for all the emulsions we studied. These data show that there is 0.10 to 0.23 speed difference for 550 nm exposures, whereas it is 1.24 to 1.33 for 750 nm exposures. If we use arithmetic units, it is only a factor of about 1.5 between vacuum and room air exposure conditions for 550 nm exposure, but it is a factor of about 20 for 750 nm exposure.

Table 2. Room Air Desensitization

	Δ Relative Log E[a]					
λ, nm	2S	4S	7S	15S	2SA	7SA
400	0.06	0.08	0.08	0.08	0.08	0.04
550	0.17	0.22	0.23	0.20	0.10	0.10
600	0.51	0.61	0.61	0.49	0.40	0.32
650	0.88	0.98	0.95	0.80	0.74	0.55
700	—	1.05	1.07	0.97	—	—
750	—	1.27	1.24	1.33	—	—

[a]Log E speed of room air exposure - Log E speed of vacuum exposure.

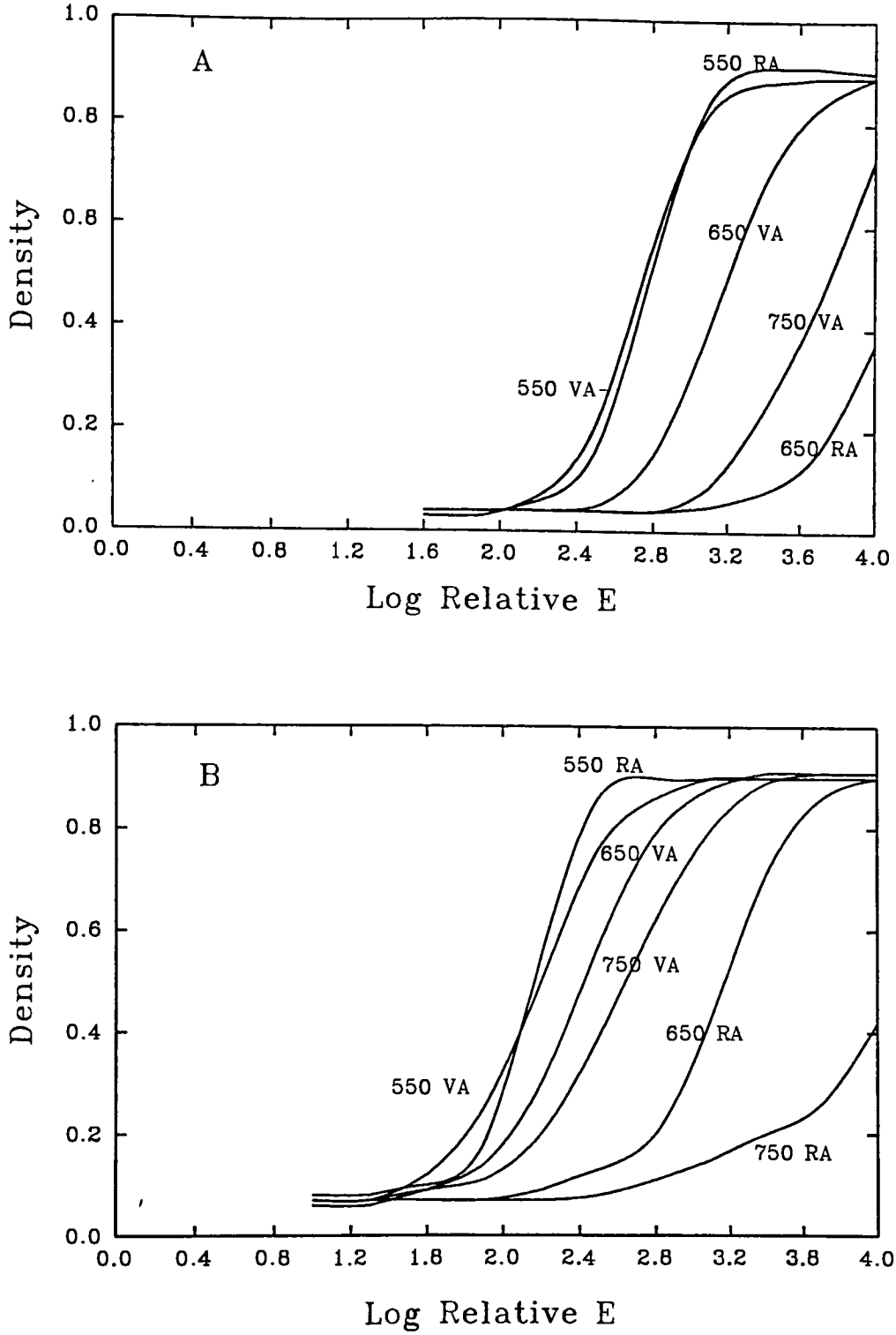

Figure 3. Effect of environmental desensitization on long wavelength speed at room temperature. A --- 2S sample; B ---15S sample. VA --- vacuum exposure condition; RA --- room air exposure condition.

This significant desensitization effect at longer wavelength sensitivity suggests that oxygen is reducing the yield of conduction band electrons. The desensitization would probably influence our temperature dependence studies of the long wavelength sensitivity if we carried them out in room air. Thus, in order to focus on the energy levels of the sensitizer centers, we conducted our temperature dependence studies on vacuum outgassed coatings.

3.2. LIRF and Long Wavelength Sensitivity. Since the temperature dependence of long wavelength sensitivity necessarily involves low intensity (narrow band filter) and long time exposure (64 to 512 seconds), it is important to understand the relationship between LIRF and wavelength. These measurements were done at room temperature using room air and vacuum outgassing conditions. The LIRF exposure design is listed in Table 3. From this design, we

Table 3. LIRF Exposure Design

blue		550 nm cutoff		600 nm cutoff	
Intensity (ND)	Time (sec)	Intensity (ND)	Time (sec)	Intensity (ND)	Time (sec)
2.0	3	0	20	0	40
3.0	30	1.0	200	1.0	400
4.0	300	2.0	2000	2.0	4000
5.0	3000	—	—	—	—

can see that it is impossible to perform LIRF properly for long wavelength exposures by using narrow band filters since extremely long exposure times would be needed.

The LIRF results of the 2S sample for blue, 550 nm and 600 nm cutoff filters are shown in Figures 4, 5 and 6. The speed difference between vacuum exposed samples and room air exposed samples also reflects the room air desensitization effect. Based on our knowledge about how the environment affects reciprocity failure, oxygen and moisture should desensitize sulfur sensitized emulsion at longer time exposure region but should have little effect in the short-time exposure region.[9] Eventually, the LIRF curves for the room air and vacuum conditions should join together in the short-time exposure region. This is the case for our blue-exposed samples (Fig. 4), but not so for long wavelength exposures (Figs. 5 and 6). Rather, the vacuum and room air curves are far apart and almost parallel over the range of exposure times used. These results indicate that the shape of the reciprocity curve for vacuum exposure is similar to that for room air exposure.

3.3. The Effect of Sulfur Sensitization Levels. The influence of sulfur sensitization levels on long wavelength sensitivity of vacuum outgassed samples at room temperature is shown in Figures 7, 8, 9 and 10. Comparing samples having different levels of sulfur sensitization, the 2S sample shows higher speed than that of the oversensitized sample (15S) at 400 nm exposure (please see Fig. 7). As the exposure is extended into the longer wavelength region,

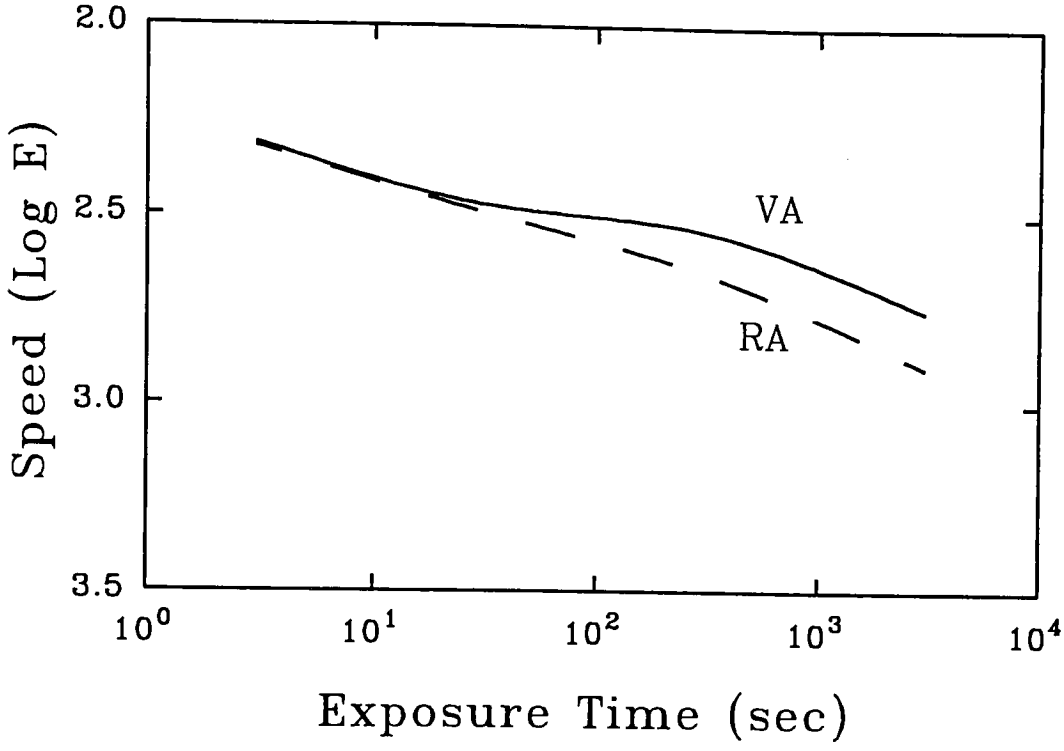

Figure 4. Reciprocity failure curves for 2S sample exposed with blue filter. VA --- vacuum exposure condition; RA --- room air exposure condition.

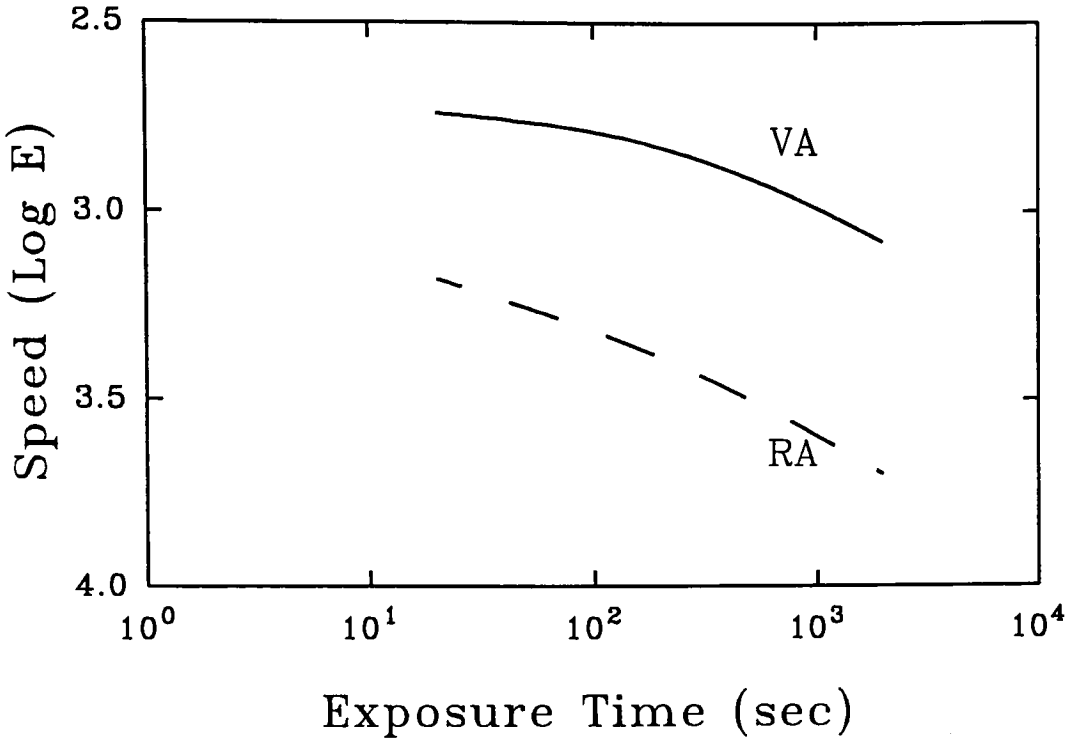

Figure 5. As in Figure 4, but exposed with 550 nm cutoff filter.

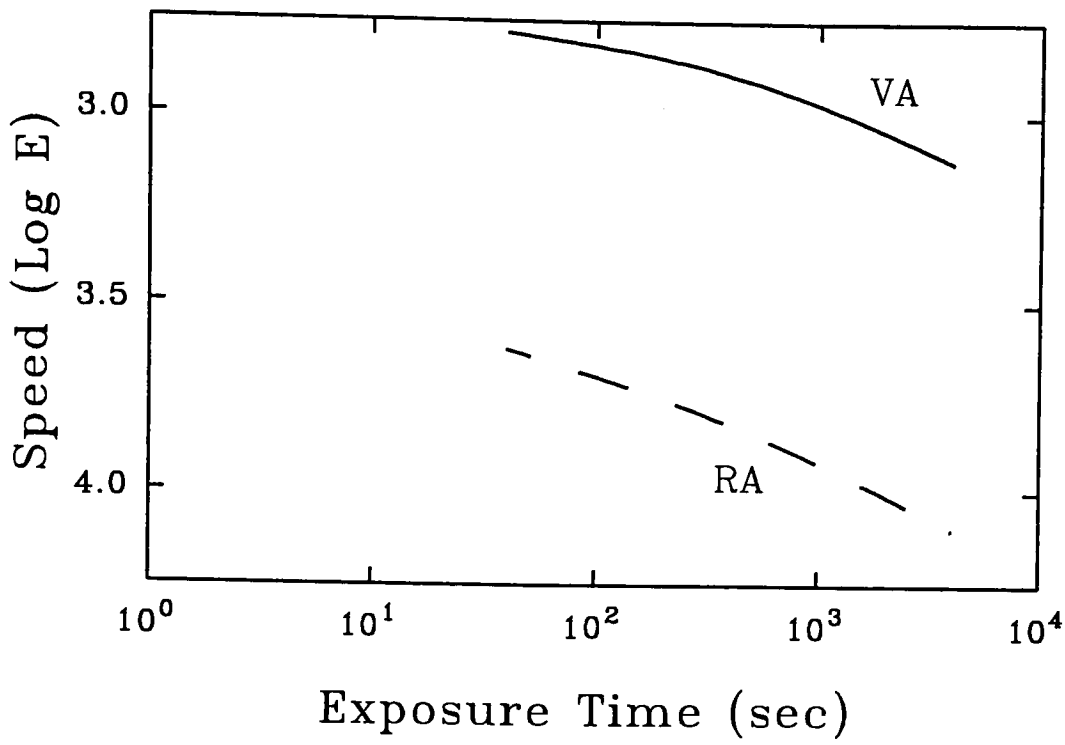

Figure 6. As in Figure 4, but exposed with 600 nm cutoff filter.

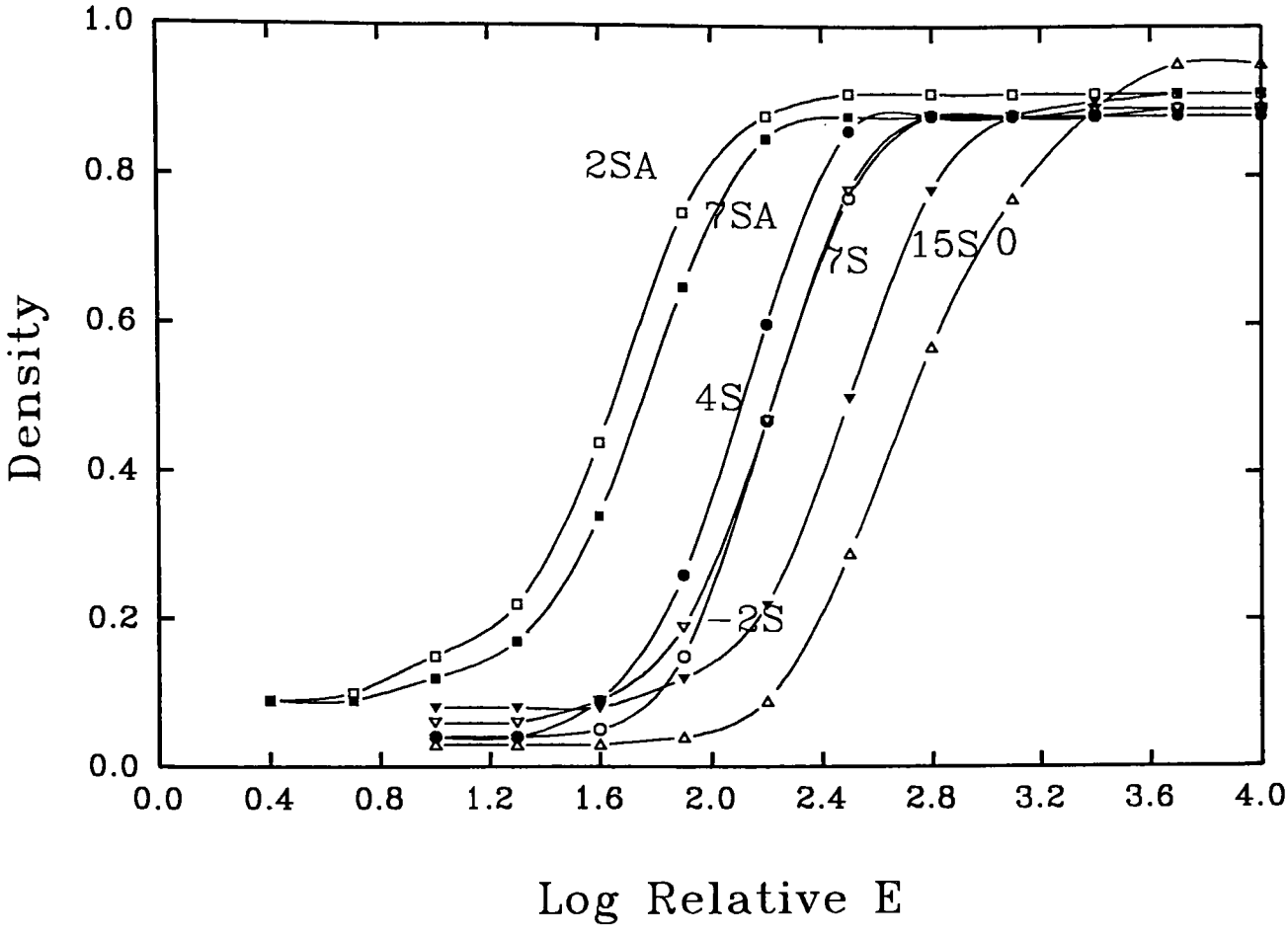

Figure 7. D-LogE curves for different sensitized samples exposed with 400 nm narrow band filter under vacuum.

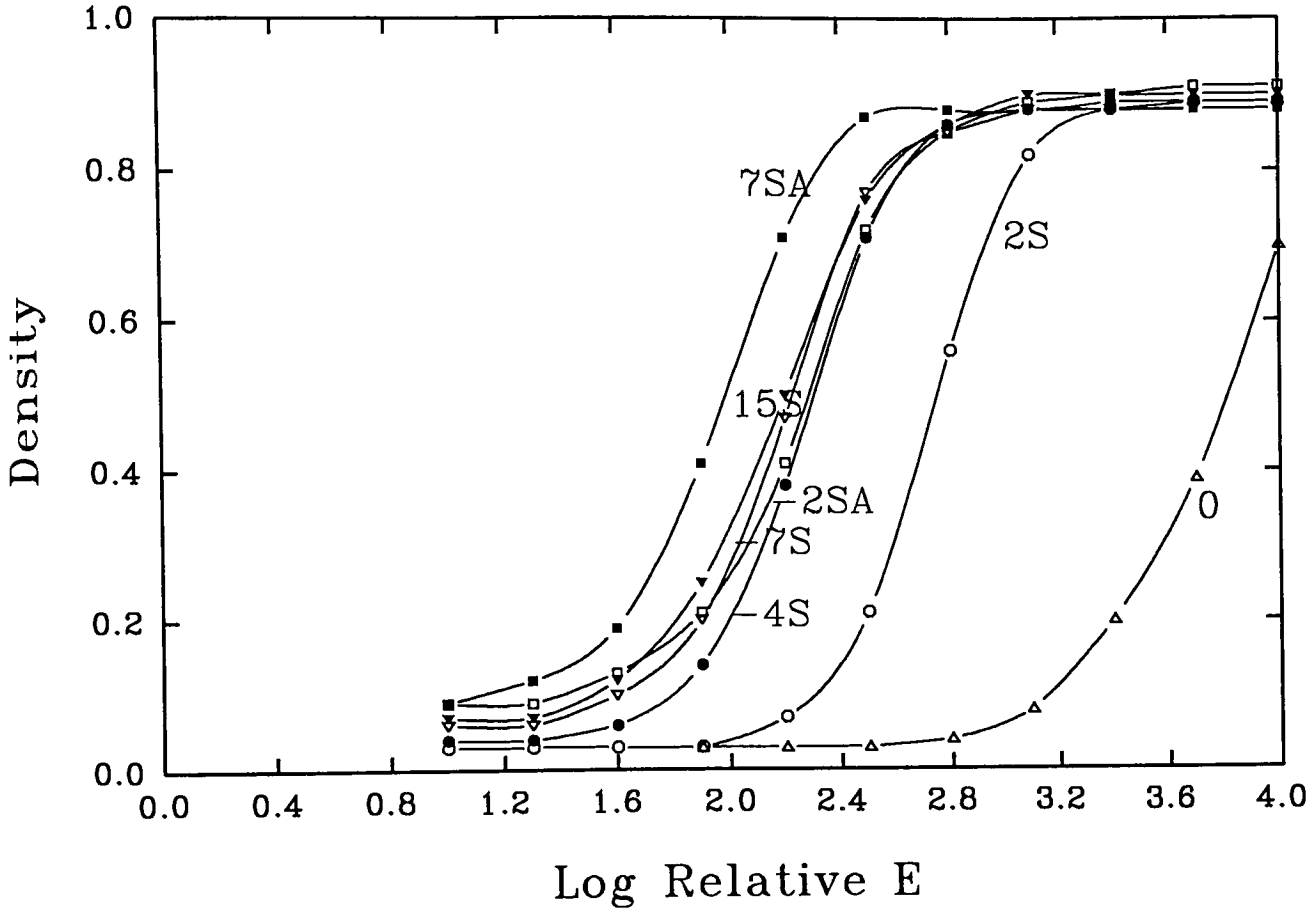

Figure 8. As in Figure 7, but exposed with 550 nm narrow band filter.

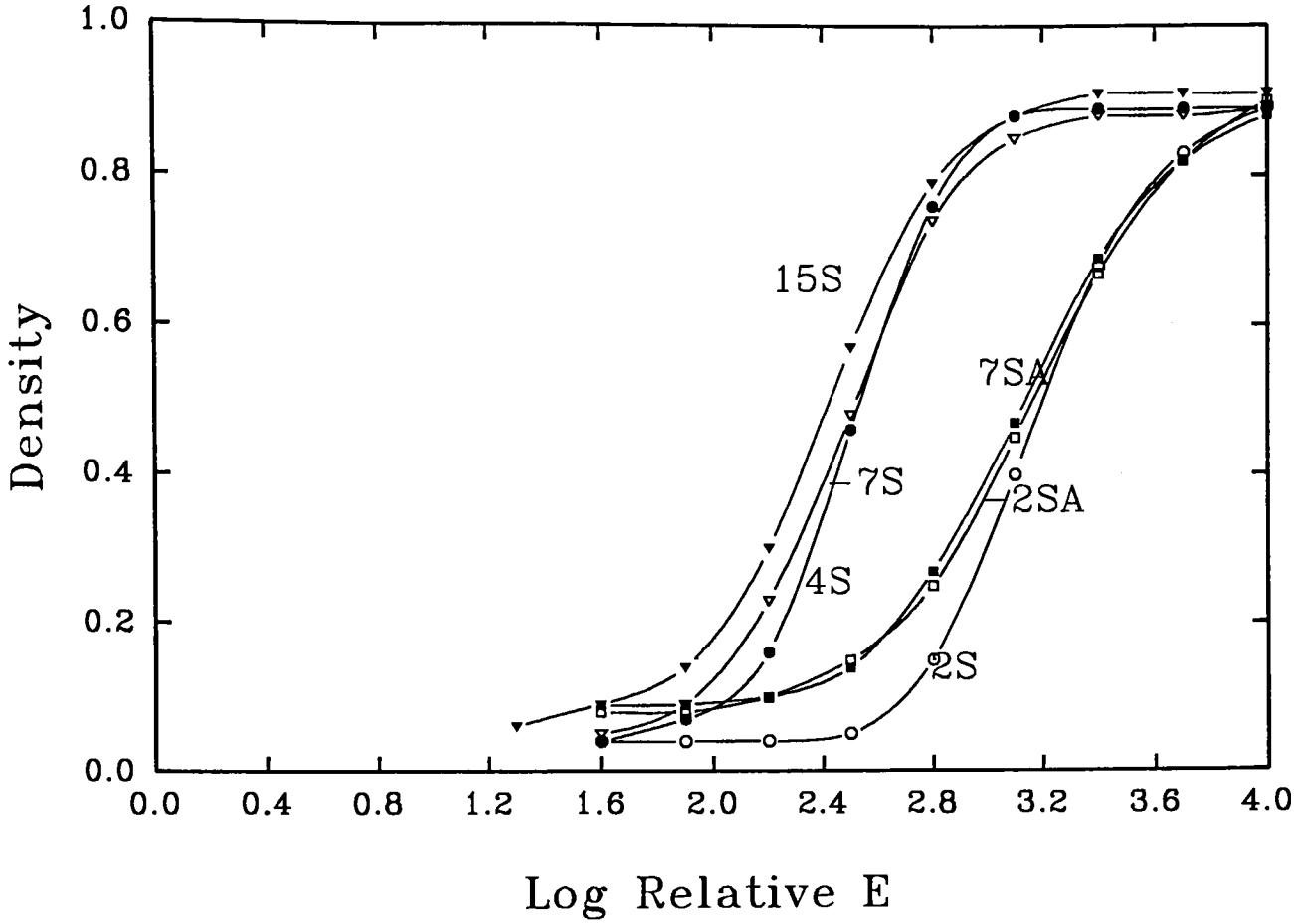

Figure 9. As in Figure 7, but exposed with 650 nm narrow band filter.

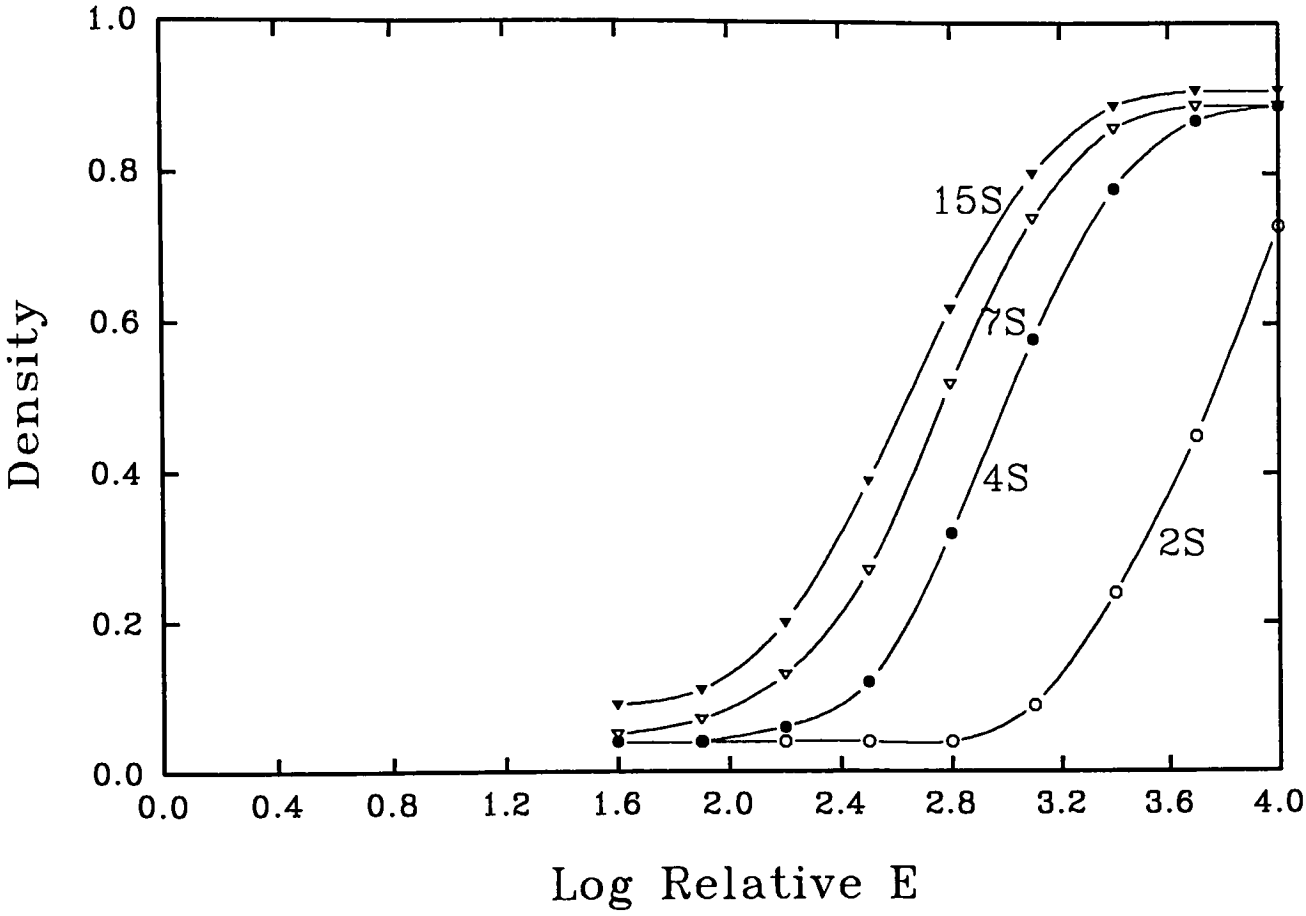

Figure 10. As in Figure 7, but exposed with 750 nm narrow band filter.

the oversensitized samples show much higher speed. At the same sulfur level, the 7S sample shows less speed than the 7SA sample between 400 and 550 nm (Fig 7 and 8) but greater speed than the 7SA sample during exposures to wavelengths longer than 600 nm (Fig. 9). It is further observed that the samples of sulfur-plus-gold sensitization showed no detectable speed at 700 nm, whereas the 15S sample exhibited relatively high sensitivity at 750 nm.

In order to study the relationship between long wavelength speed and sulfur level for sulfur sensitized emulsions, we also corrected for differences in blue speed, in incident number of photons, and in exposure time. The corrected speed versus sulfur level for each long wavelength narrow band filter is plotted in Figure 11. These curves indicate that there is an appreciable increase in speed when sulfur level is increased from 2 mg to 4 mg, but the curves become flatter when sulfur level is further increased. Note that there is some response from the unsensitized emulsion at 550 nm.

We also studied the relationship between the corrected speed and wavelength for sulfur sensitized and sulfur-plus-gold sensitized emulsions. Figure 12 is the plot for sulfur sensitization and Figure 13 is the plot for sulfur-plus-gold sensitization. For sulfur sensitization, all curves of speed versus wavelength appear parallel and indicate that the speed difference is due to the difference of sulfur level. On the other hand, the curves of speed versus wavelength for sulfur-plus-gold sensitization are steeper than those of sulfur sensitization.

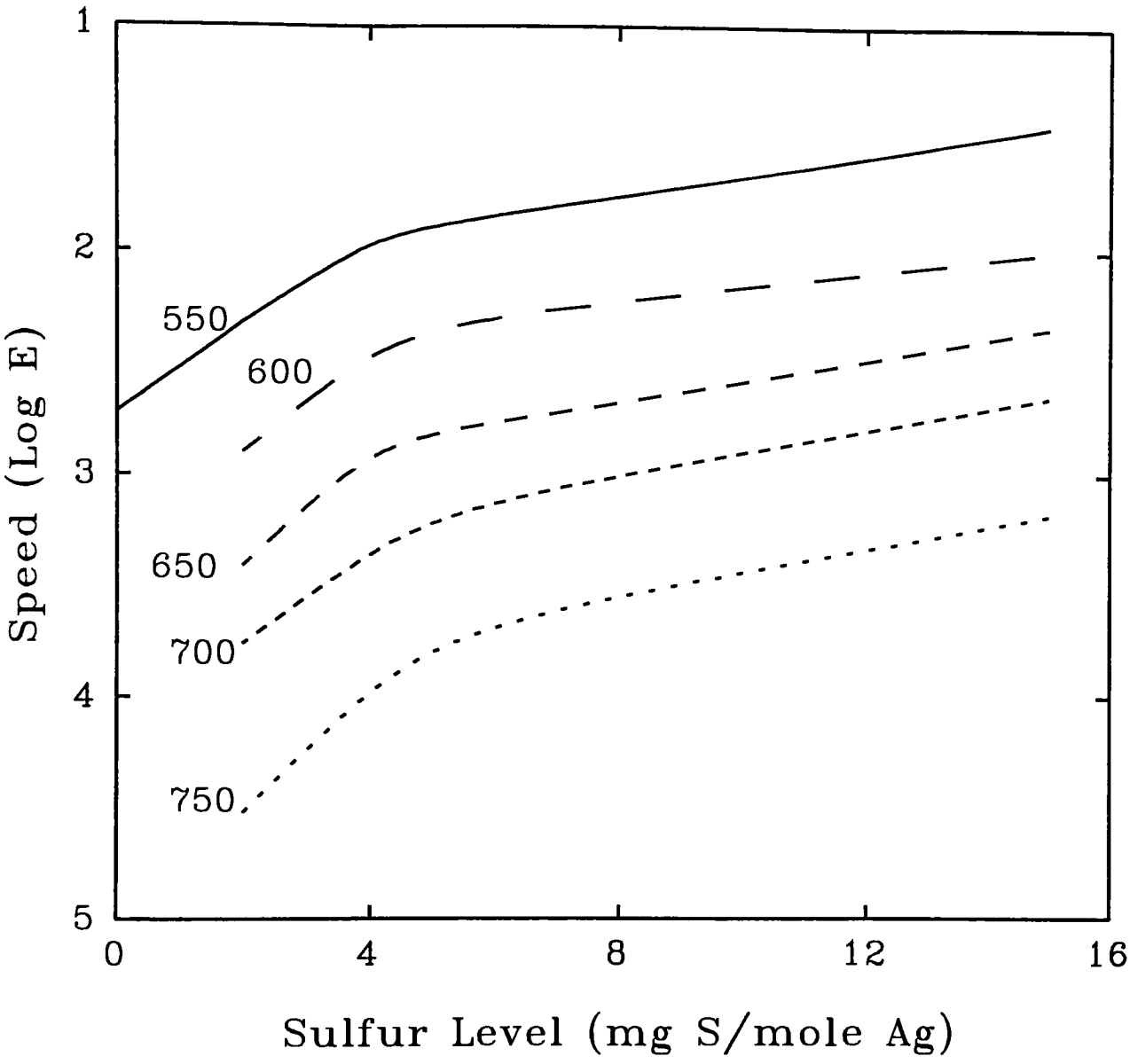

Figure 11. The relationship between the relative long wavelength speed and sulfur level for sulfur sensitized emulsions. Labels indicate exposure wavelength in nm.

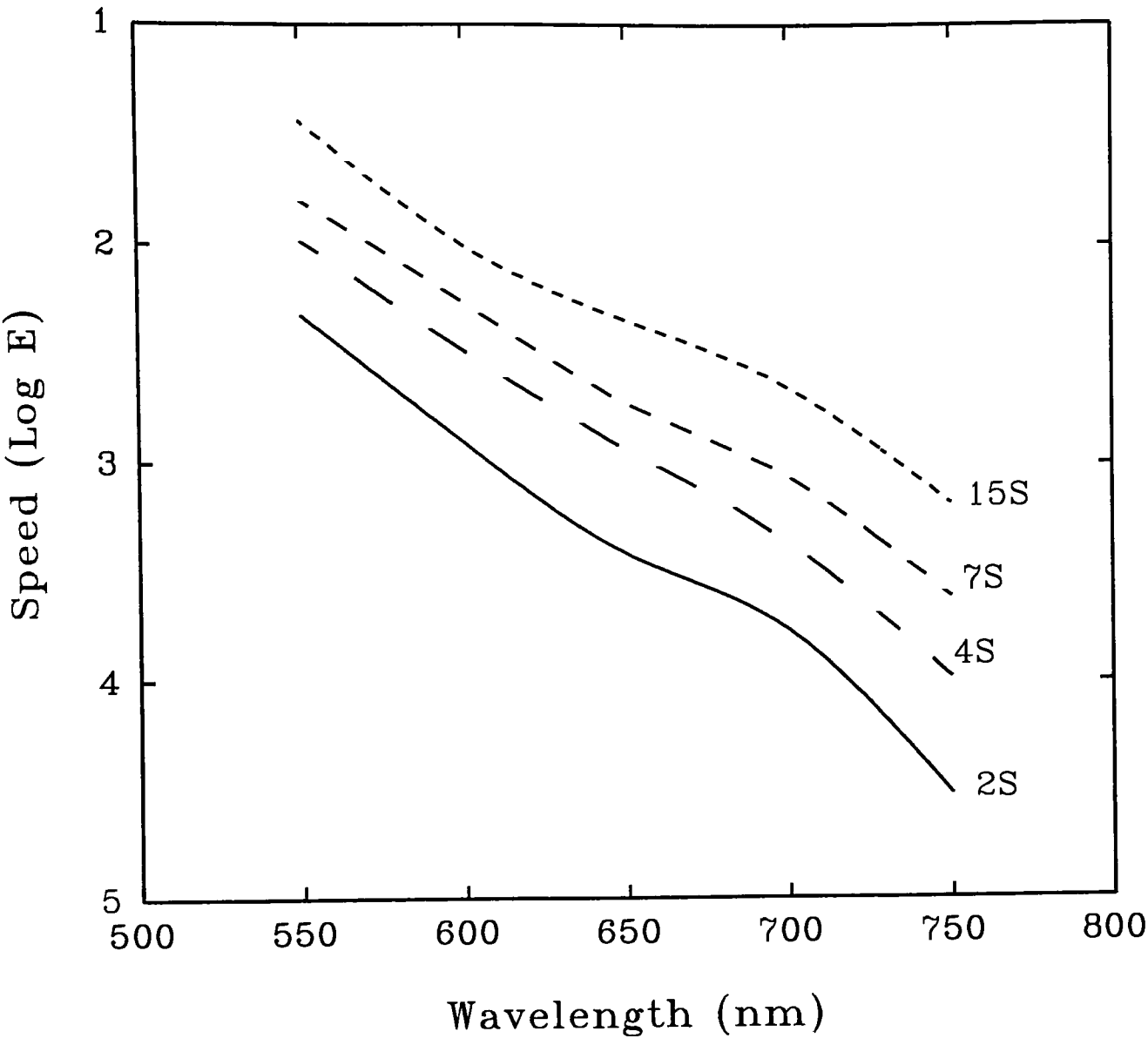

Figure 12. Speed versus wavelength plot for sulfur sensitized emulsions. Labels indicate sulfur levels.

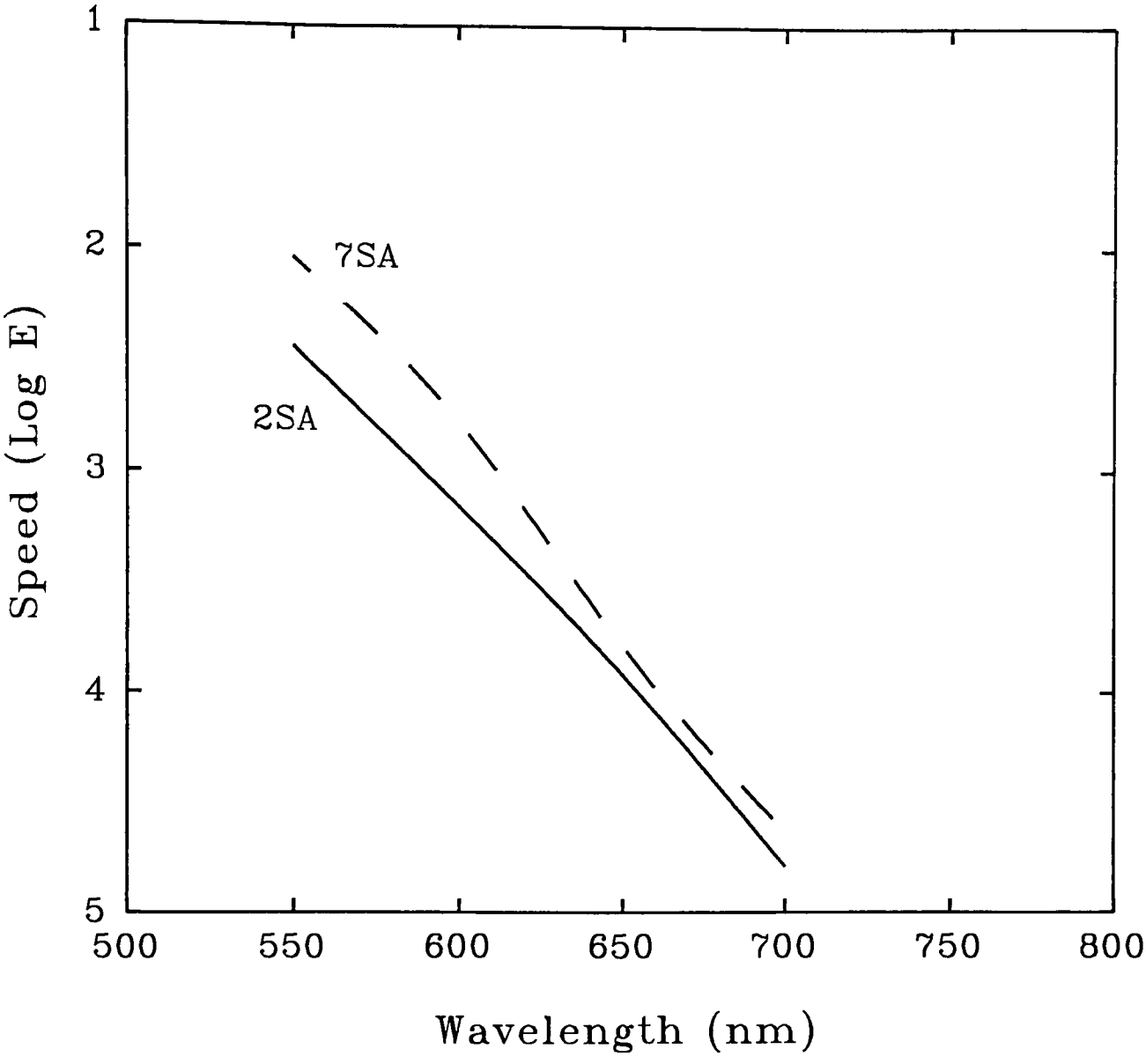

Figure 13. Speed versus wavelength plot for sulfur-plus-gold sensitized emulsions. Labels indicate sulfur-plus-gold levels.

It seems that gold in the sensitizer center destroys some long wavelength speed. This effect can be correlated with changes in absorption, as noted by Hirsch.[10]

3.4. The Temperature Dependence of Blue Light Sensitivity. For each narrow band filter, we exposed six different sensitized samples by choosing a proper exposure time. The exposure temperature varied from 25°C to -30°C. This temperature range was chosen to eliminate the possibility of thermal effects at high temperature exposure such as fog. The speed at 400 nm versus reciprocal temperature for different sulfur and sulfur-plus-gold sensitized samples is plotted in Figure 14. For the sulfur sensitized samples, an increase in sulfur level increases the slope and therefore increased the temperature dependence. For sulfur-plus-gold sensitized samples, an increase in sensitizer level does not change the slope and thus has no temperature dependence effect. At the same sulfur level, the sulfur sensitized samples show greater temperature dependence than the sulfur-plus-gold sensitized samples.

3.5. The Temperature Dependence of Long Wavelength Sensitivity. The effect of temperature on the response of the 2S and 15S coatings exposed at 650 nm is shown in Fig. 15A and 15B, respectively. The decreasing contrast with decreasing temperature was observed for many of the samples. For this reason, we measured speed at 0.15 above fog. This does mean, of course, that the activation energies will be a function of the reference density used to measure speed. We corrected the long wavelength speeds for

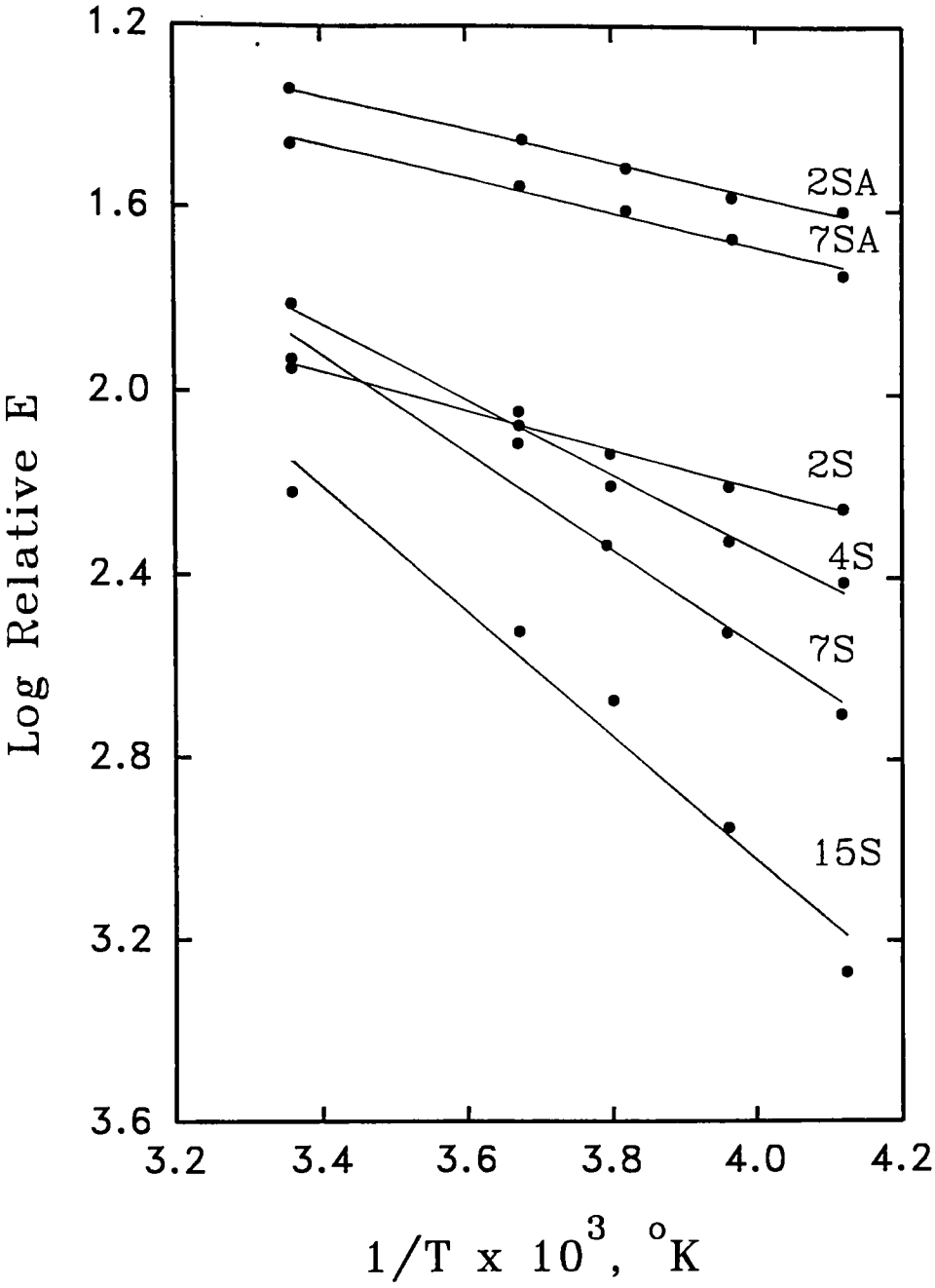

Figure 14. The temperature dependence of blue light sensitivity for sulfur and sulfur-plus-gold sensitizations.

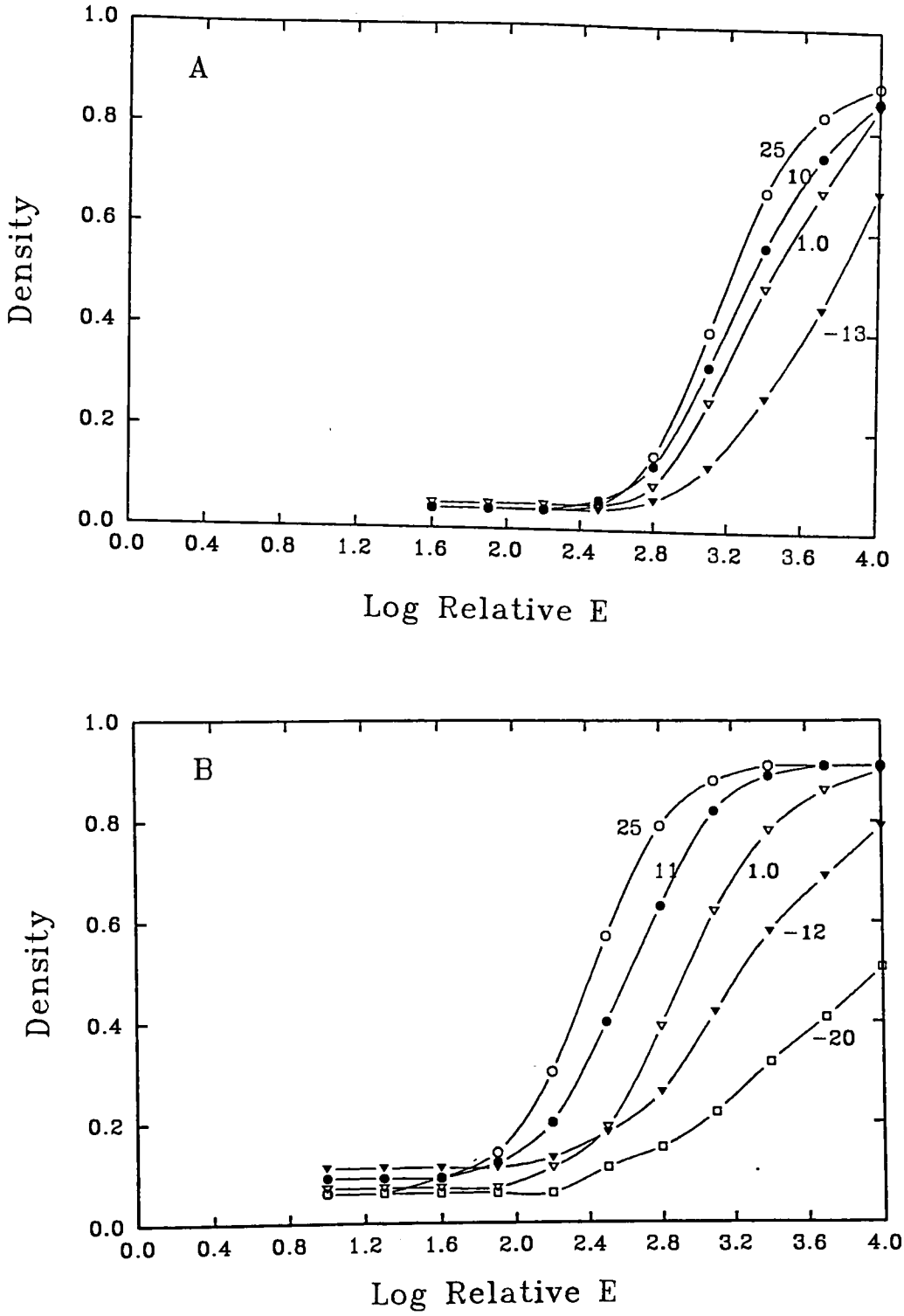

Figure 15. D-Log E curves showing temperature dependence of 650 nm sensitivity. Labels are exposure temperature in °C. A --- 2S coating; B ---15S coating.

exposure time and incident photon density differences by using the speed and intensity of the 550 nm narrow band exposure as the reference. These corrected speeds at each wavelength are plotted against reciprocal temperature in Figure 16.

For sulfur sensitization, as the exposure wavelength increases, the sensitivity decreases and temperature dependence increases. For example, the 2S coating has less temperature dependence at each wavelength than the 4S coating (Figs. 16A and 16B, respectively). For sulfur-plus-gold sensitization (Figs. 16E and 16F), as the exposure wavelength increases, the sensitivity decreases dramatically but the temperature dependence increases only slightly. At the same sulfur level, the sulfur-plus-gold samples showed much less temperature dependence effect than the corresponding sulfur only samples. Clearly, speed at each wavelength and its temperature dependence both increase as the level of sulfur sensitization increases. When the exposure wavelength is extended toward the red, the temperature dependence increases.

3.6. Activation Energies. Equation(1) was used to calculate apparent activation energies from the plots in Figures 14 and 16. These data are summarized in Table 4. Several trends emerge. First, for any wavelength, the apparent activation energy increases with increasing level of sulfur sensitization. Second, for any level of sulfur sensitization, the apparent activation energy increases with wavelength shift towards the red. Third, at the same level of sulfur,

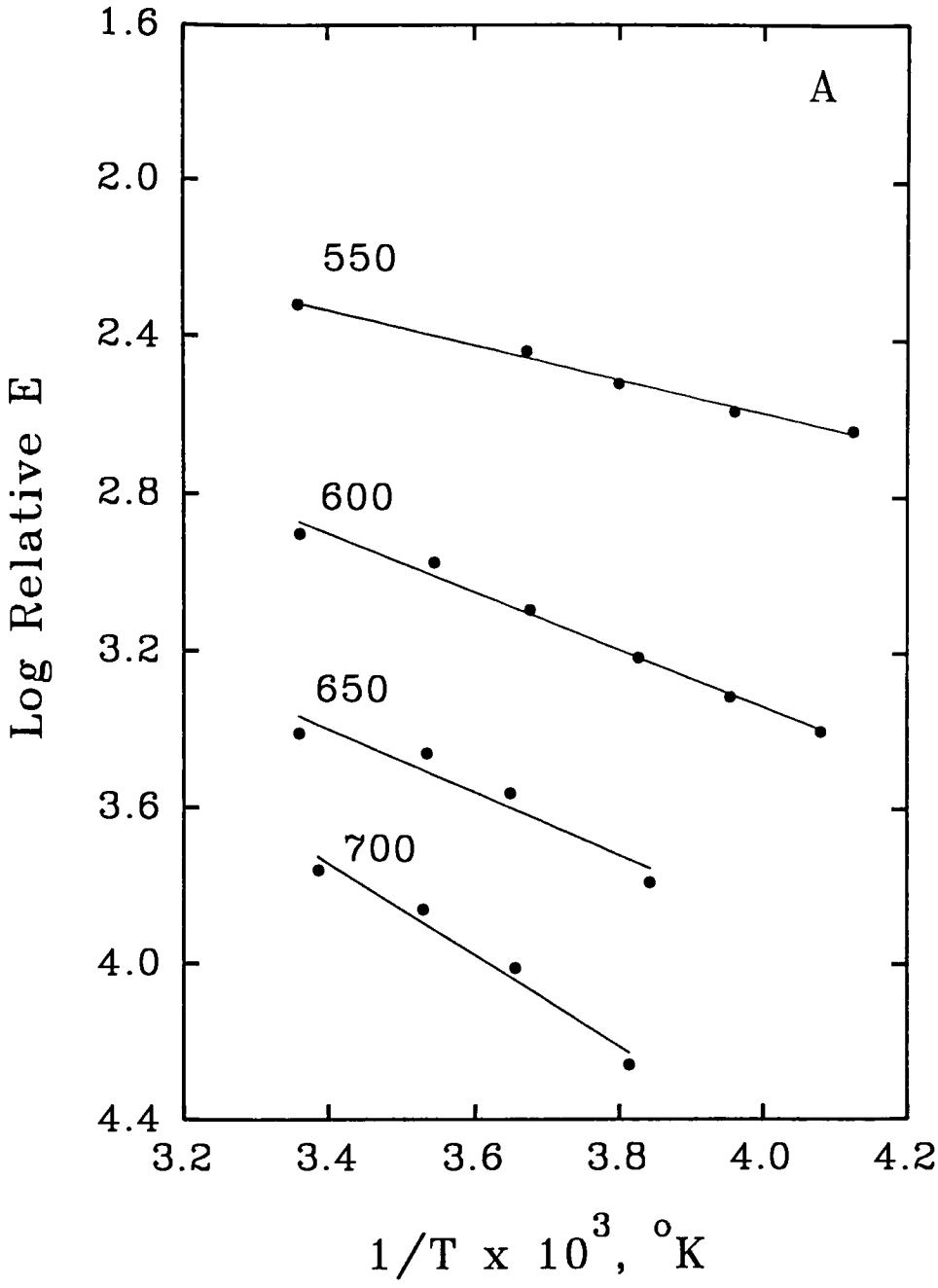

Figure 16. The temperature dependence of long wavelength sensitivity from 25°C to -30°C. 550 --- 550 nm narrow band filter; 600 --- 600 nm narrow band filter; 650 --- 650 nm narrow band filter; 700 --- 700 nm narrow band filter; 750 --- 750 nm narrow band filter. A --- 2S sample; B --- 4S sample; C --- 7S sample; D --- 15S sample; E --- 2SA sample; F --- 7SA sample.

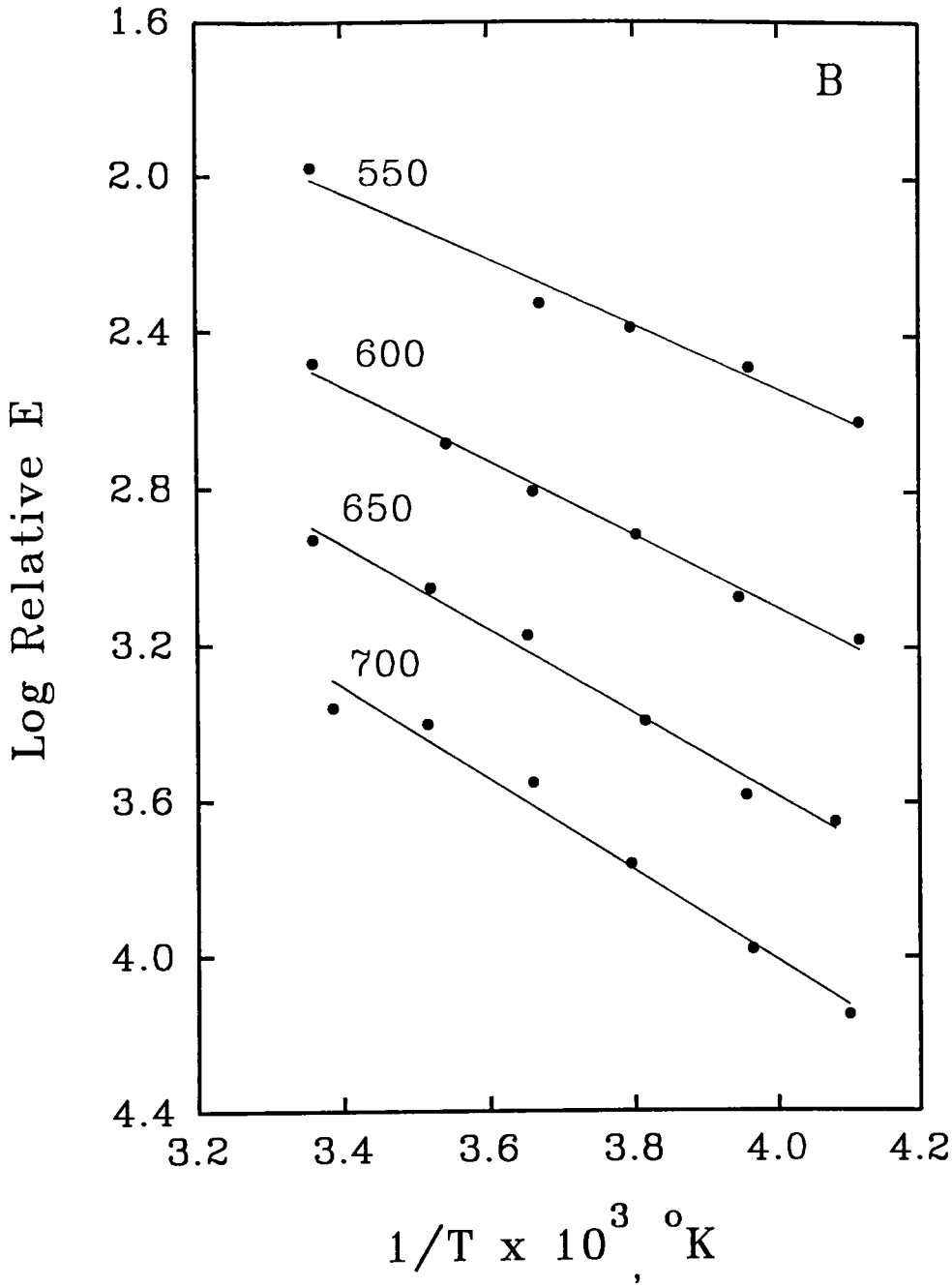
B
550
600
650
700
1.6
2.0
2.4
2.8
3.2
3.6
4.0
4.4
3.2
3.4
3.6
3.8
4.0
4.2
Log Relative E
1/T x 10^3, °K

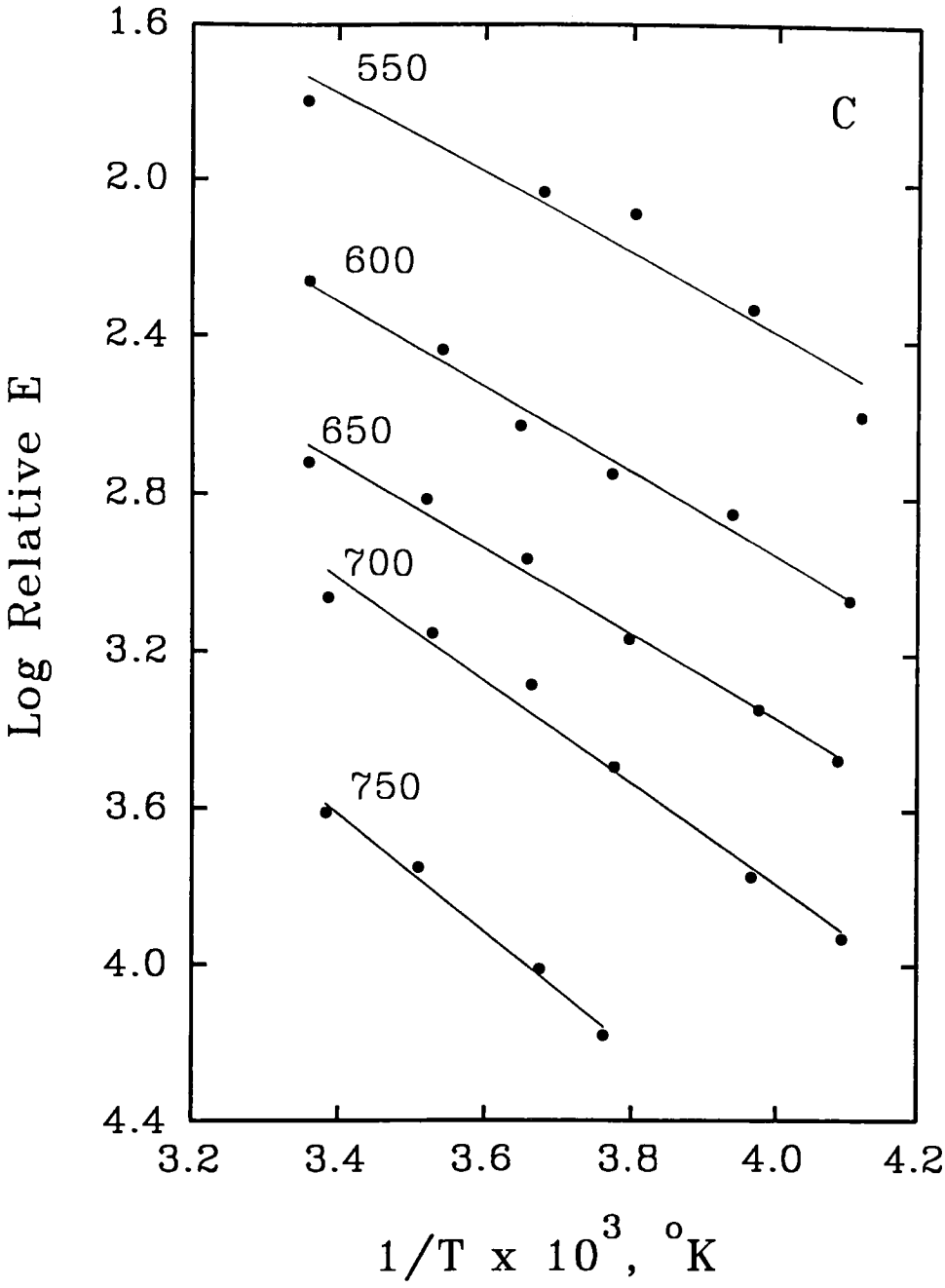
1.6
2.0
2.4
2.8
3.2
3.6
4.0
4.4
550
600
650
700
750
C
Log Relative E
3.2
3.4
3.6
3.8
4.0
4.2
1/T x 10^3, °K

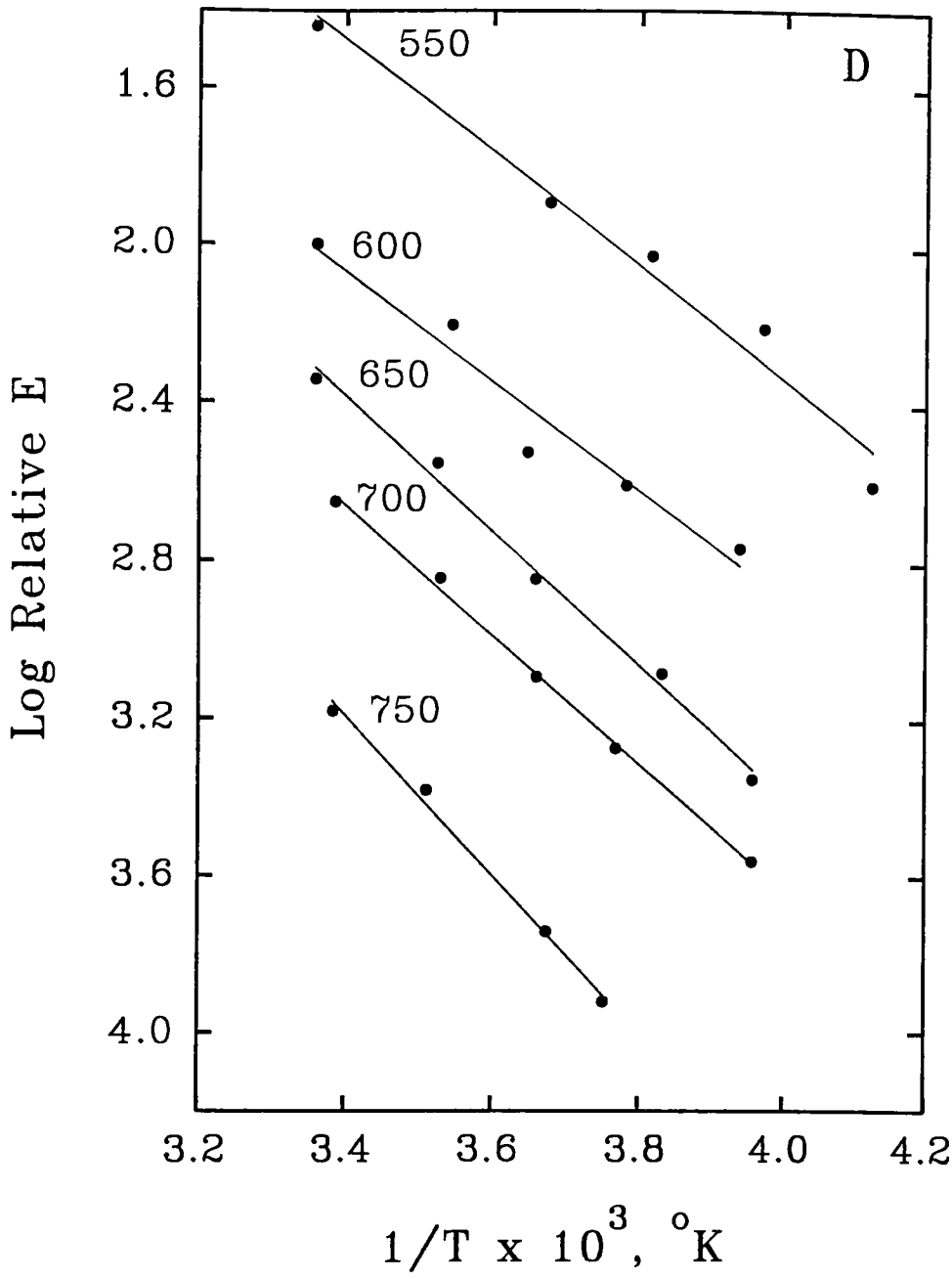
550
600
650
700
750
D
1.6
2.0
2.4
2.8
3.2
3.6
4.0
Log Relative E
3.2
3.4
3.6
3.8
4.0
4.2
1/T x 10^3, °K

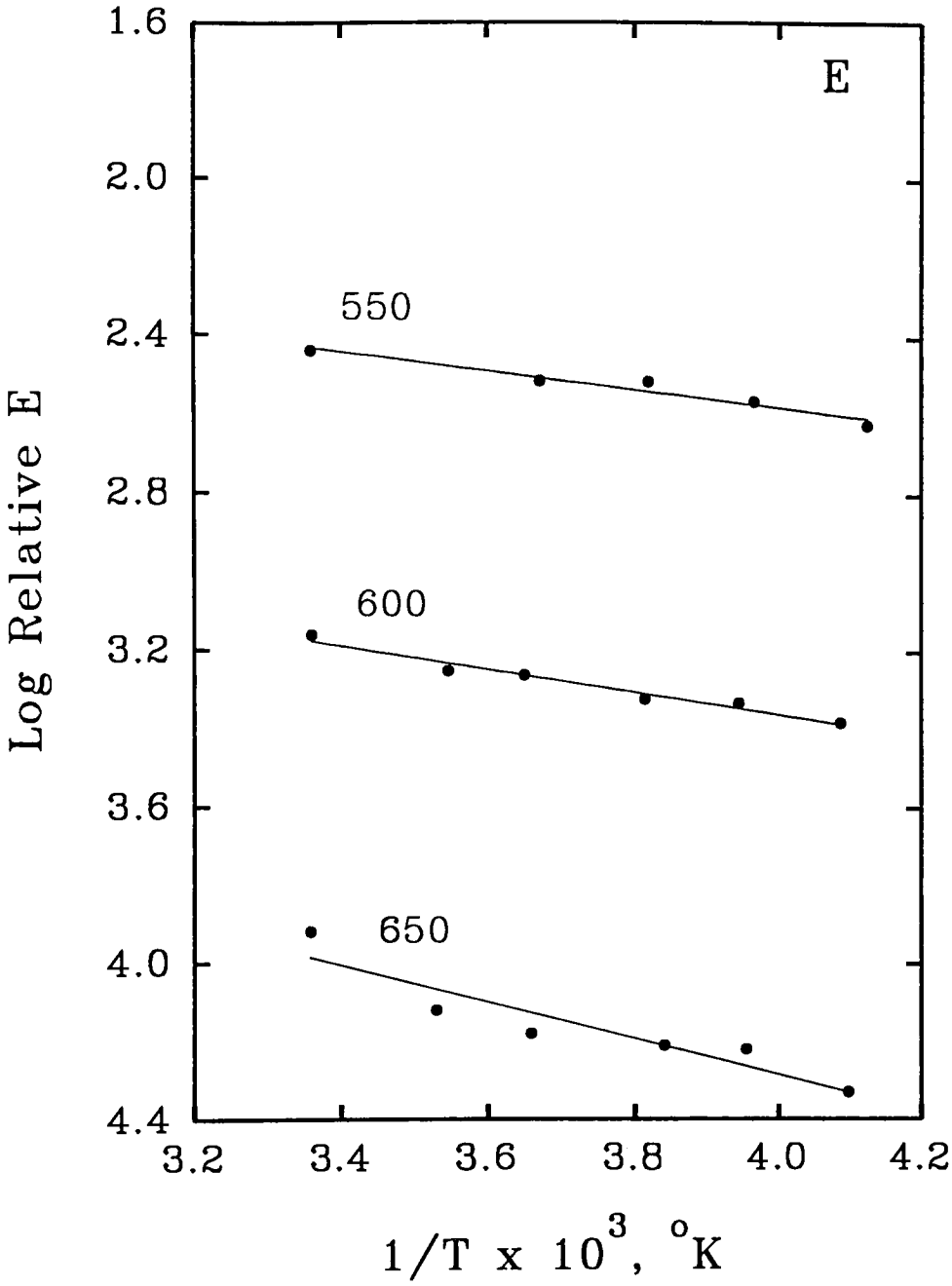
E
550
600
650
Log Relative E
1.6
2.0
2.4
2.8
3.2
3.6
4.0
4.4
3.2
3.4
3.6
3.8
4.0
4.2
1/T x 10^3, °K

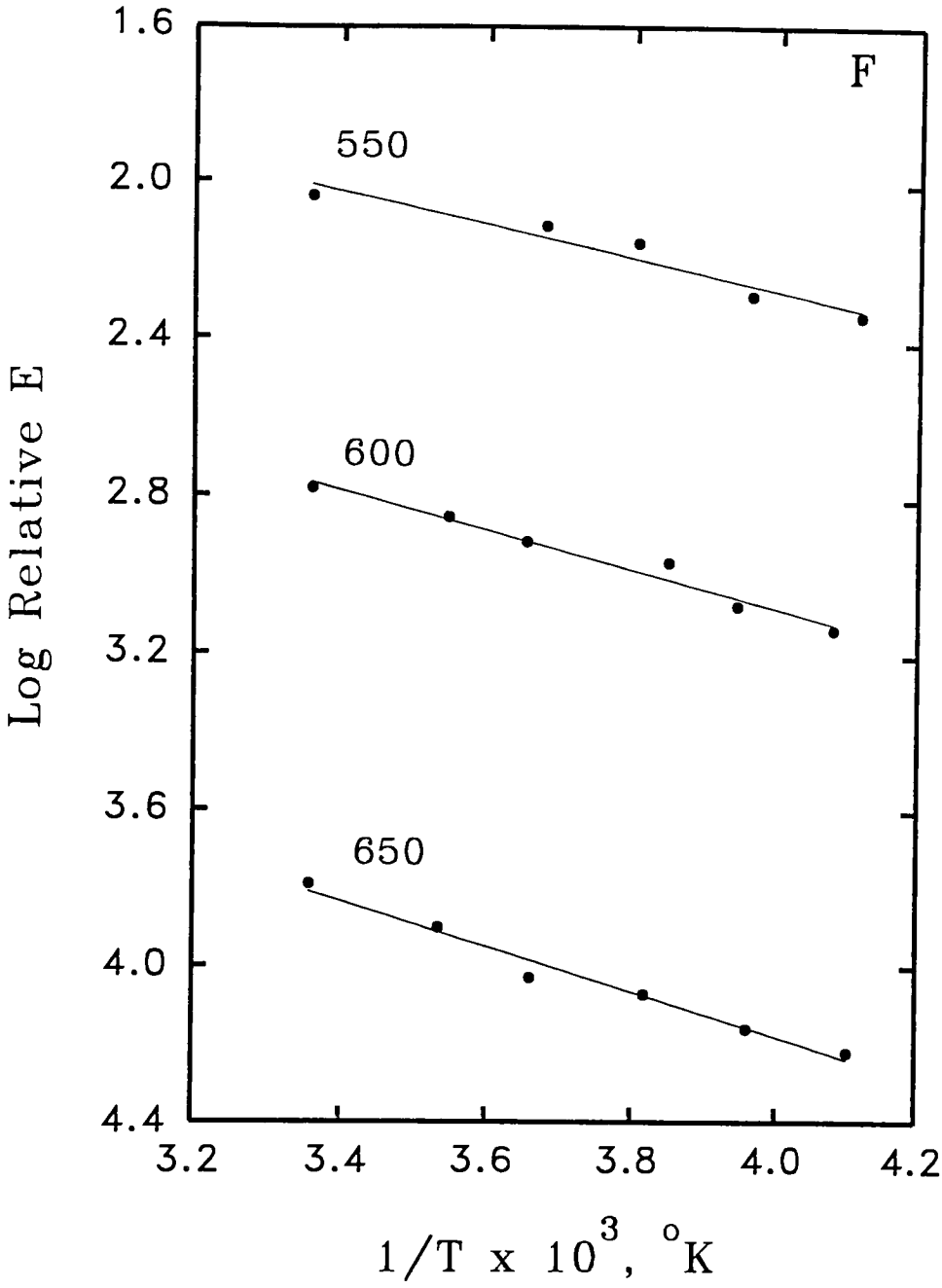
F
550
600
650
1.6
2.0
2.4
2.8
3.2
3.6
4.0
4.4
3.2
3.4
3.6
3.8
4.0
4.2
Log Relative E
1/T x 10^3, °K

the apparent activation energies for sulfur-plus-gold sensitization were less than those for sulfur sensitization.

Hailstone[11] measured the temperature dependence of light absorption by AgBr microcrystals and found an "activation energy" of about 0.02 eV for 400 nm light absorption in the temperature range 25°C to -75°C. This "activation energy" must be subtracted from the 400 nm values in Table 4 to obtain the true activation energy, i.e., that due to the effect of temperature on the processes involved in latent-image formation.

Table 4. Apparent Activation Energies[a]

	ΔE, eV					
λ, nm	2S	4S	7S	15S	2SA	7SA
400	.08±.01	.16±.02	.21±.04	.27±.06	.07±.01	.07±.01
550	.08±.01	.16±.03	.20±.06	.28±.03	.04±.01	.08±.03
600	.14±.02	.18±.01	.21±.03	.27±.07	.06±.01	.10±.02
650	.16±.09	.21±.02	.21±.02	.33±.03	.09±.04	.11±.02
700	.23±.06	.23±.05	.26±.04	.32±.02	—	—
750	—	—	.30±.04	.40±.05	—	—

[a]Uncertainties reflect the 2σ error limits from the least squares fit of the Log E vs 1/T plots.

We assume that once an electron is in the conduction band that the temperature dependence of latent-image formation will be independent of the source of the electron — 400 nm or long wavelength. Therefore, we must subtract the apparent activation energy of the 400 nm results, after correction for the temperature dependence of 400 nm absorption, from that of the long wavelength results to obtain a thermal energy which is relevant to the energetics of the long wavelength response, ΔE_{act}. These results are summarized in Table 5.

Table 5. Activation Energies ---- Blue Corrected[a]

	ΔE_{act}, eV					
λ, nm	2S	4S	7S	15S	2SA	7SA
550	.02±.01	.02±.04	.01±.07	.03±.08	0	.03±.03
600	.08±.02	.04±.02	.02±.05	.02±.09	.01±.01	.05±.02
650	.10±.09	.07±.03	.02±.04	.08±.07	.04±.04	.06±.02
700	.17±.06	.09±.04	.07±.06	.07±.06	—	—
750	—	—	.11±.06	.15±.08	—	—

[a]Uncertainties derived from the expression $\mu_{corr} = (\mu_{400}^2 + \mu_\lambda^2)^{1/2}$, where μ_{400} is the uncertainty at 400 nm, μ_λ is the uncertainty at long wavelength λ, and μ_{corr} is the uncertainty of the blue corrected result.

In one case, 2SA at 550 nm, the correction resulted in a ΔE_{act} that was less than zero, so we have simply placed a "0" in the table for this situation. In several cases there is zero or negative activation energy when the experimental uncertainties are considered. Therefore, there is some probability that the activation energy is negative at short wavelengths and changes to positive when exposure wavelength extended to longer wavelength region. Further work with more precise measurements is needed to reduce the experimental uncertainties and to verify that the activation energy could be negative. Further explanations for the possibility of negative activation energy occuring in this thesis will be given in discussion section.

From Table 5, we notice that the activation energies still tend to increase with increasing wavelength, but now no longer tend to increase with increasing sensitization level. Those for the 2SA coating are less than for the 2S coating, but the opposite is true for the 7S and 7SA coatings.

IV. DISCUSSION

In this work we study the electronic properties of sensitizer centers produced by sulfur and sulfur-plus-gold sensitization. Previous work using a similar approach made some very specific interpretations, namely, that the temperature dependence for long wavelength sensitivity, when corrected for the temperature dependence of the blue response, is a measure of the trap depth associated with sensitizer centers. There are several problems with

this interpretation which we now discuss in light of the results presented in this thesis.

4.1. Environmental Desensitization. We have found a significant increase in the long wavelength response when the coatings are given a 16-hour vacuum outgassing. Improvements in photographic response by vacuum outgassing are well known, primarily because of the work of James and his coworkers.[9] The proposed mechanism for this effect is electron transfer to O_2 from a crystal trap site or from a dye trap site if a sensitizing dye is present.[12] This is thought to be a reversible transfer and the final fate of the electron is determined by whether or not a hole is present to recombine with the electron trapped at the O_2 molecule. Evidence to support this proposal comes from the small sensitivity of reduction-sensitized emulsions to vacuum outgassing.

Hamilton has proposed an alternative mechanism for the effect of vacuum outgassing.[13] He suggests that O_2 is chemisorbed on the surface and blocks the intrinsic hole removal sites. This would explain the pronounced effect that vacuum treatment has on LIRF. Computer simulations[13] based on the nucleation-and-growth model of latent-image formation show that incorporating a hole removal event mimics to a very good degree the effect of vacuum outgassing. On the other hand, an electron removal event or enhanced recombination does not mimic the vacuum effect.

Thus, a very characteristic feature of vacuum outgassing is its effect on low-intensity reciprocity failure (LIRF) and a small to vanishing effect at higher intensities. This is exhibited in Figure 4 for blue exposures of the 2S coating. In contrast, the long wavelength exposures show a quite different effect (Figs. 5 and 6). Here the sensitivity increase in vacuum is large, but is only weakly dependent on intensity. It seems that the desensitization mechanism of O_2 is quite different in these two spectral regions. In fact, Hamilton's simulation of the two vacuum effect mechanisms is remarkably like the results in Figs. 4, 5, 6. In the case of O_2–blocked hole traps, the simulated reciprocity failure looks like that of Fig. 4, whereas in the case of electron removal by O_2, the curves look like those of Figs. 5 and 6.

If a long wavelength exposure causes an electron to be injected into the conduction band via the excited state of the sensitizer center, then the interaction between this electron and O_2 should be quite similar to that for an electron produced in the conduction band by an intrinsic exposure. Changes in LIRF due to vacuum outgassing should not depend on the spectral region of exposure. This is contrary to our experimental observations. This suggests that we are dealing with a different mechanism of O_2 desensitization in the long wavelength region.

We propose that O_2 is scavenging electrons before they can be injected into the conduction band by a long wavelength exposure. This mechanism is not sensitive to the rate of generation of the electrons, i.e., the intensity of exposure. Because we do not know the

lifetime of the excited state of the sensitizer center, it is difficult to judge whether or not quenching of the excited state is possible. Our estimate is that it is improbable. The situation being discussed here is similar to that for O_2 desensitization of spectral sensitization. The energy level of the dye is crucial in determining the extent of desensitization. As the LV level of the dye moves further from the vacuum reference the desensitization by O_2 increases.[11,12c] If the excited state of the dye were being quenched by O_2, then there would not be an energy level dependence for this desensitization. The more usual interpretation is that a long-lived state (the trapped electron) is produced, allowing for transfer to O_2. We believe these considerations are applicable to our situation.

A more likely situation is that the hole in the ground state of the excited sensitizer is injected into the valence band, resulting in an electron trapped at a sensitizer center. This trapped electron may then be thermally excited into the conduction band, recombine with a mobile hole, or be scavenged by a diffusing O_2 molecule which may serve as a recombination center for the mobile hole.

In their study of long wavelength sensitivity, Hamilton and coworkers found that the sensitivity was appreciably enhanced by the presence of a hole-trapping dye. This is similar to the effect of vacuum outgassing we have found. Indeed, the two results support a common mechanism. Even though O_2 would still be present, a hole-trapping dye would reduce the number of holes available for permanent loss of the electron via recombination. Such a dye would mimic the effect of reduction sensitization.

4.2. Activation Energies. First of all, we notice that the uncertainties in our activation energies are such that a negative activation energy is possible (550 nm and 600 nm values, Table 5). Explanations for such a possibility fall into several categories. The first two relate to possible changes in our simple mechanism for latent image formation caused by absorption in the long wavelength region. The third possibility derives from the realization that our measurements are the net results of many steps in latent image formation. Relating the measured activation energy to a single step is a difficult and complicated procedure.

Negative activation energies discussed in the literature[14] are attributed to multi-step reactions in which one step is exothermic. If the exothermicity is greater than the energy required for the thermally activated step, then the observed activation energy will be negative. Applying this mechanism to our situation, we could envision the photon absorption by the sensitizer center leading to an excited state from which an exothermic decomposition or rearrangement may occur. A thermal activated electron transfer step then may occur from this new state. The exact mechanism by which this decomposition or rearrangement may occur is not known. However, if this mechanism is operative in our system, then the measured activation energies will not relate simply to the energy levels which we are trying to determine.

An alternative explanation for the possible negative activation energies relates to the unknown electronic properties of the sensitizer center. It is possible that the absorption coefficient of these centers increases with decreasing temperature. In either case the effective concentration of excited sensitizers increases as temperature is decreased and this may act to offset a decrease in the rate of electron transfer with decreasing temperature. This would lead to a zero activation energy if the two processes exactly offset each other or to a negative activation energy if the rate of increase in the concentration of excited sensitizer centers was greater than the decrease in rate of electron transfer. If this is true, the measured activation energies will be less than the energy difference between the sensitizer center levels and the electronic levels of the AgBr.

The third possible explanation relates to the way in which the activation energies are calculated. The activation energies for the long wavelength sensitivity are calculated by subtracting the activation for the intrinsic exposure from that for the long wavelength exposure. There are two possible problems with this method. First, there is a difference in the reciprocity failure characteristics between a long wavelength and an intrinsic exposure. This difference may lead to a difference in activation energies that that is not corrected for by the simple subtraction described above. Second, as noted earlier, the activation energy for the long wavelength response is a function of the reference density at which the speed is taken. This is due to a temperature-dependent contrast in the case of long wavelength exposures that is not seen for intrinsic

exposure. This again suggests that our subtraction method for calculating the activation energy may be too simplified. If either of these explanations is true then our activation energies are, again, not simply related to the energy levels we are trying to measure.

Now let us turn to the measured activation energies. A critical question to be answered is: What process do they relate to? The situation here is similar to that experienced in spectral sensitization studies. In both cases we are producing latent image by less than bandgap irradiation. The common view in this case is that, from the excited state, either the electron or hole is transferred to either the conduction or valence band, respectively.[15] The complementary carrier remaining in the sensitizer center can then transfer to the AgBr grain in a time period determined by the energy difference between its state and the energy of the pertinent band, either conduction or valence.

The critical part of this process is the separation of the electron and hole, otherwise the electron will return to the ground state and no effect will be produced. As to whether electrons or holes are transferred in the initial step, this is determined by the energy levels of the sensitizer center relative to those of silver bromide. The position of these energy levels may be such that some thermal assistance is needed in the first step of the process. We will adopt the view, as have others, that any measured activation energy for this sensitization will relate to this first critical step.[11,16] Any additional

thermal energy for release of the complementary carrier will probably not be reflected in our measurements.

So, let us now try to answer the question posed above. From Table 5 we note that there is essentially no thermal activation required for exposure at 550 nm. One possible approach then is to position the lowest vacant level of the sensitizer center at or above that associated with the conduction band threshold. Longer wavelength exposures require some activation energy, so we would position the lowest vacant levels for the sensitizer centers absorbing in these regions slightly below the conduction band threshold.

If we adopt this model, however, we find an inconsistency with the results of our environmental study. In Table 2 we note that the sensitization by vacuum outgassing for exposures at 550 nm is greater than that for exposure at 400 nm. If the lowest vacant level of the sensitizer centers giving rise to the 550 nm absorption were at or above the conduction band threshold, the result of vacuum outgassing should be similar for 400 nm and 550 nm exposures.

To further illustrate the inconsistencies, we can look for a correlation between the degree of environmental desensitization and the activation energy. If we use blue-corrected data for both we should find that a linear regression fit should extrapolate to the origin. That is, when the activation energy is zero, the environmental desensitization for the long wavelength response should be no different than that of the intrinsic response. Such a plot is given in

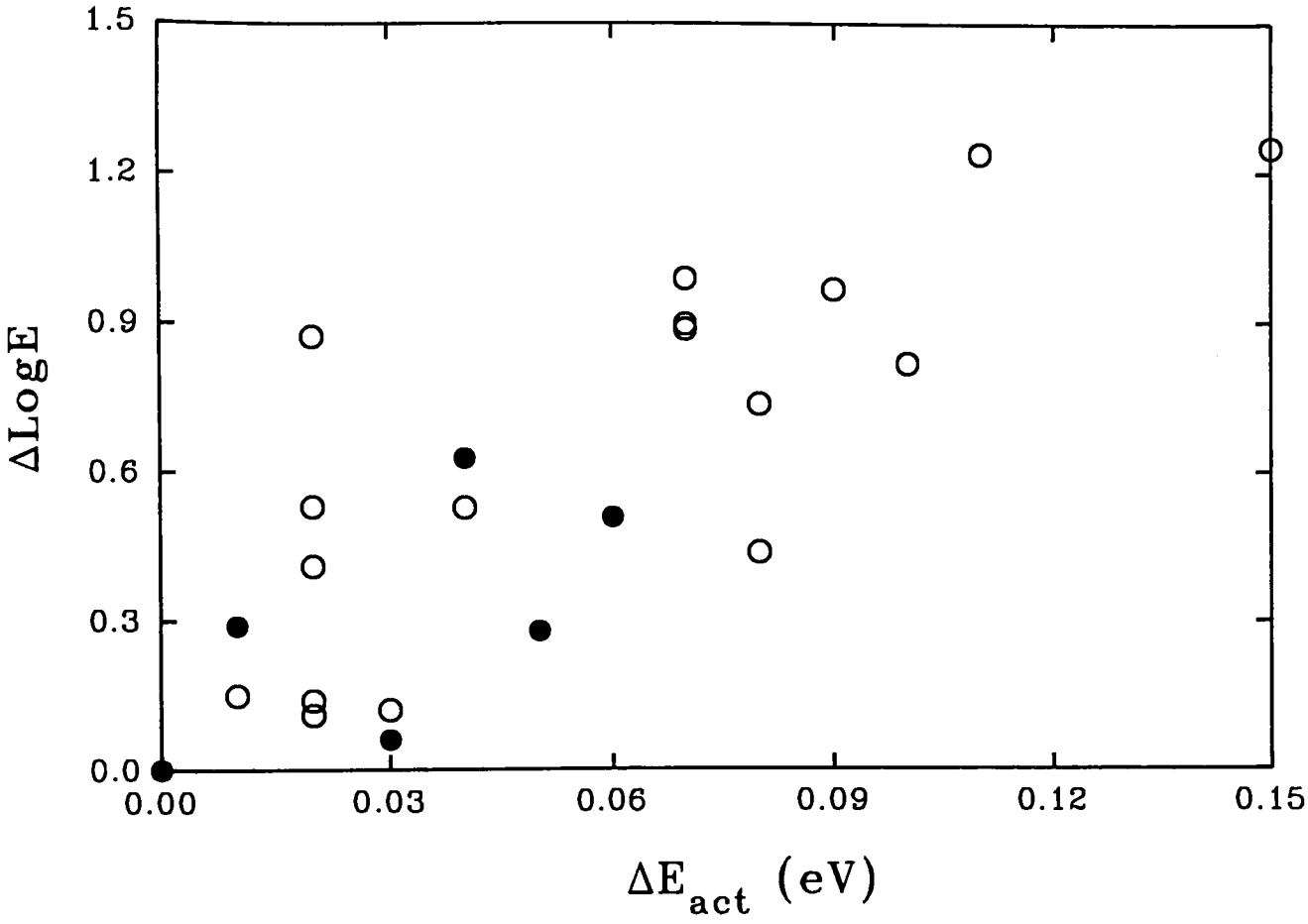

Figure. 17. Environmental desensitization vs activation energy. o, sulfur sensitized; •, sulfur-plus-gold sensitized.

Fig. 17. We have grouped our data independent of sensitizer level, distinguishing only between sulfur and sulfur-plus-gold sensitized samples. Because the data used in Fig. 17 are not overly noisy, the scatter-plot nature of this figure suggests that the correlation sought is inappropriate, i.e., the model is not correct.

We propose that our activation energies are measuring the thermal energy required to inject a hole into the valence band from the excited state of the sensitizer center. In the case of the 550 nm exposure we would position the ground state of the sensitizer center at the valence band maximum. This would position the lowest vacant level within the bandgap, the energy below the conduction band threshold being determined by the assumed energy bandgap of AgBr. With this energy level picture, excitation of the sensitizer center would lead to injection of a hole into the valence band and the formation of a trapped electron at the sensitizer center. This trapped electron could be thermally assisted into the conduction band or it could be lost to recombination with a valence-band hole. In a room air exposure it could also be scavenged by O_2 molecules as we discussed above.

Using this proposed model, we have built an energy level picture for all our data and present it in Fig. 18. For the AgBr bandgap we have used 2.6 eV, as proposed by Berry.[17] It must be admitted that this is somewhat arbitrary for we observed photographic response in the unsensitized emulsion at 550 nm (2.24 eV). The ground states of the sensitizer centers have been positioned

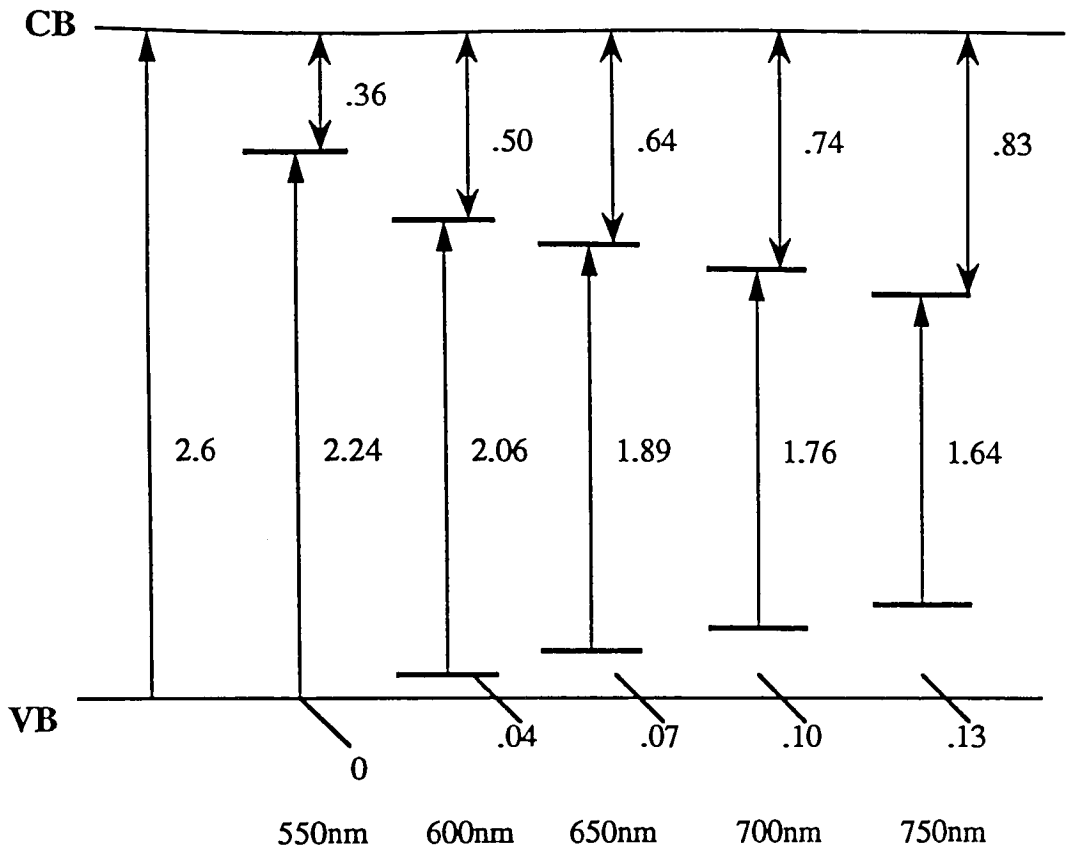

Figure 18. A proposed model of energy levels of sulfur sensitizer centers. Labels are in eV's.

above the valence band by an amount equal to the average values for the activation energies at each wavelength from Table 5. To this position we add the energy of the photon at that particular wavelength to arrive at the position of the lowest vacant level i.e.,

$$E_{photon}(eV) = 1234/\lambda(nm) \qquad (2)$$

Because of the arbitrariness of the AgBr bandgap energy, the energy difference between the lowest-vacant level and the conduction band is somewhat imprecise and should not be taken as quantitative.

As we mentioned above, in this proposed model, we assume that the electron transfer in the sulfur sensitization is similar to that of spectral sensitization. The highest-filled molecular orbital (HF) of sensitizer center is occupied by electrons in the ground state. Absorption of visible light by the sensitizer center excites one of the electrons in HF to LV, the lowest-vacant level in the ground state, without changing its spin, yielding a molecule in the first excited singlet state. In the Huckel approximation[18] the transition energy between the ground and first excited singlet state is equal to the energy difference between the levels LV and HF.

Since the composition, the size and the size distribution of sensitizer centers are unknown, the molecular orbital of sensitizer centers could not be drawn like single triatomic molecules. But from the spectral absorption spectrum of bulk silver sulfide, we know that the energy difference between HF and LV of bulk silver sulfide is

about 0.9 eV. We also know that the sulfur sensitizer centers are some kind aggregates of $(Ag_2S)_n$ with n at least 3. It is reasonable to expect that the splitting and overlapping of the molecular orbital of a multiple-molecular aggregate will cause the energy bandgap smaller than that of a single molecule. Therefore, the energy levels of sulfur sensitizer centers will fall in the range between that energy levels of single molecule and bulk of silver sulfide. The explanation for wavelength dependence of energy level of sensitizer center will be presented further in the chapter of Spectral Distribution of Long Wavelength Response.

This energy level picture fits our environmental desensitization data. It predicts that as the exposure wavelength increases it should produce electrons more deeply trapped within the bandgap. These electrons would have a longer time to be scavenged by O_2 and, therefore, the longer wavelength exposures should show the greatest sensitivity to O_2. This is consistent with our data summarized in Table 2.

At this point we discuss other possible electronic transitions that could be induced by the long wavelength exposure. It may be possible for an absorbed photon to cause a transition from the valence band of the AgBr to the lowest-vacant level of the sensitizer center. In this situation an electron trapped at the sensitizer center is created and any measured activation energy would be related to its electron trap depth — the energy we desire. However, if this were the case, we would expect a much better correlation between the

environmental desensitization and ΔE_{act} (Fig. 17). Another possible transition is from the highest-filled level of the sensitizer center to the AgBr conduction band. In this case, no activation energy for long wavelength sensitivity is expected, contrary to what we observe experimentally.

4.3. Comparison with Earlier Work. The discrepancy between our measurements and those of Hamilton and coworkers can now be addressed. There are several differences in experimental arrangement, but the main one is the environment in which the activation energies were measured. Hamilton and coworkers used room air conditions with controlled relative humidity. Thus, their results must have been influenced by the O_2 desensitization we have documented in this paper. If our energy level scheme is essentially correct, then the transfer of electrons from the trapped electron level to O_2 will compete with the thermally assisted transfer to the conduction band. As the temperature is lowered and the electron spends more time trapped at the sensitizer center, there will be an increasing chance for transfer to O_2. Thus, the falloff in speed by lowering the temperature will be increased in room air and the activation energy will be correspondingly higher.

Although there are undoubtedly other differences between our work and that of Hamilton and coworkers, such as sensitizer level and exposure wavelength, the environmental difference is the key to explaining the different activation energies. For example, we carried out some preliminary temperature dependence measurements with

cutoff filters like that used in the previous work and found activation energies very similar to those in Table 5. We see no clear effect of sensitizer level on activation energy, so this difference is probably not important.

Hamilton and coworkers also measured the activation energy in the presence of a hole trapping dye. They found the activation energy to be somewhat smaller than those without the dye present. This would be consistent with our energy level scheme because the hole-trapping dye would reduce the chance of permanent electron loss through reaction of the hole with O_2^-. The activation energies with the dye present are still considerably larger than our values. This is probably because the O_2^- radical is very reactive and may react with other species in the coating. Our technique of vacuum outgassing provides a much better solution to the interference by O_2.

4.4. Relation to Trap Depths. Even if one accepts our proposed energy level picture, the depicted energy levels may not be the critical ones in the photographic process. This is because we are interested in the energy level, or more precisely the trap depth, of an electron located at the sensitizer center. What we show in Fig. 18 are the levels *before* electron trapping. The level after electron trapping may lie higher than, or lower than, or even be similar to the level before trapping. Hamilton has postulated that there is a lattice relaxation upon the trapping of an electron so that the trap depth becomes greater than that indicated by the lowest vacant level in Fig. 18.[19]

At this point we return to our attempts to find a correlation between environmental desensitization and activation energy (Fig. 17). Given our proposed energy level scheme in Fig. 18, we see that the environmental desensitization for the long wavelength response should be at least proportional to the energy gap between the lowest vacant level and the conduction band, ΔE_{gap}. The equation for calculating ΔE_{gap} is

$$\Delta E_{gap} = 2.6 \text{ eV} - E_{photon} - \Delta E_{act} \qquad (3)$$

where E_{photon} is the photon energy. Figure 19 shows that when this variable is used as the abscissa, a much better correlation with environmental desensitization is achieved. This provides support for our model of the energy levels of sensitizer centers.

Upon further inspection of Figure 19, we find that the intercept on the ΔE_{gap} axis is not zero, but rather 0.29 ± 0.06 eV for the sulfur samples and 0.34 ± 0.09 eV for the sulfur-plus-gold samples. Since the regression fit should pass through the origin, this means that the energy levels of the trapped electrons must lie about 0.3 eV *higher* than the lowest vacant levels depicted in Figure 18.

The reason for this required shift in LV level is due to one or several of the following considerations. First, we have already mentioned that the bandgap energy (2.6 eV) is imprecise and could be smaller than indicated in our scheme. This would decrease all the gaps between the lowest vacant levels and the conduction band

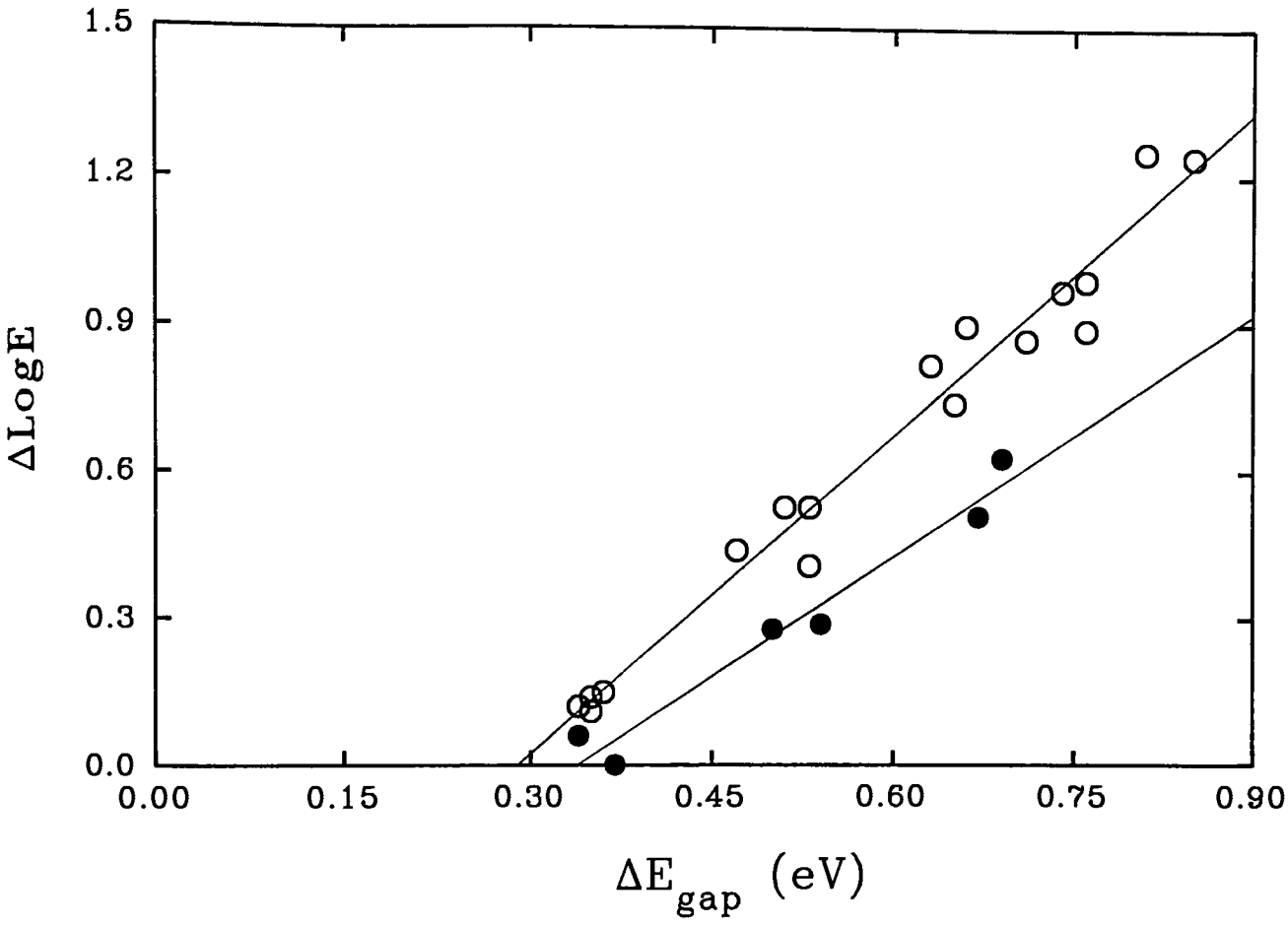

Figure. 19. Environmental desensitization vs the energy gap between the lowest vacant level and the conduction band. Symbols as in Fig. 17. Lines are a linear regression fit of the data.

minimum equally. Second, the energy levels of the electron may shift upwards, with respect to the lowest vacant level, when it is trapped at the sensitizer center. Finally, our activation energies may be related to hole transfer to a surface state, rather than to the valence band. Whatever the reason, our analysis suggests that the trapped electron state is about 0.05 to 0.50 eV below the conduction band minimum for the sensitizer centers absorbing in the range 550 to 750 nm.

Although the abscissa intercepts in Fig. 19 are not different at the 2-sigma uncertainty level, the trend does appear to be dependent on sensitization type. The higher value for the sulfur-plus-gold sensitized samples suggests that trapped electrons in these sensitizer centers would lie slightly higher in energy (about 0.05 eV) than those for the corresponding sulfur sensitizer centers absorbing at the same wavelength. The slopes of the two linear regression fits in Fig. 19 are just distinguishable at the 2-sigma uncertainty limit. This difference is unexpected from our simple picture where environmental desensitization is only dependent on the energy level of the trapped electron and suggests the situation may be more complicated.

We have calculated the thermal trap depths for electrons, ΔE_{therm}, for each sensitizer level and each wavelength using the following equation

$$\Delta E_{therm} = \Delta E_{gap} - E_{shift} \qquad (4)$$

where E_{shift} is obtained from the abscissa intercepts in Fig. 19. These values are summarized in Table 6. We have used two different values for E_{shift}, depending on whether the sample is sensitized with sulfur or sulfur-plus-gold. Because our uncertainties are in many cases large, the data in this table can only be used to establish trends. There is a distribution of thermal trap depths for both types of sensitization, but it is much broader for the sulfur sensitized samples. Our data indicate little effect of sensitizer level.

Table 6. Thermal Trap Depths for Electrons

	ΔE_{therm}, eV					
λ, nm	2S	4S	7S	15S	2SA	7SA
550	.06±.06	.06±.07	.07±.09	.05±.10	.03±.09	0±.09
600	.18±.06	.22±.06	.24±.08	.24±.11	.20±.09	.16±.09
650	.34±.11	.37±.07	.42±.07	.36±.09	.35±.09	.33±.09
700	—	.45±.07	.47±.08	.47±.08	—	—
750	—	—	.56±.08	.52±.10	—	—

4.5. Spectral Distribution of Long Wavelength Response. It has been suggested that there must be an aggregation of Ag_2S molecules on the grain surface before there can be an enhancement in photographic sensitivity by sulfur sensitization[20]. Thus, it might be expected that there is a distribution of different size silver-sulfide clusters present on the grain surface. Since bulk silver sulfide has a bandgap in the infrared, it is reasonable to expect a trend in excitation energy such that larger clusters require lower energy. The distribution of cluster sizes may favor the smaller ones since these are precursors to larger ones. These smaller size clusters would absorb at the shorter wavelengths.

The long wavelength speed will be determined by two factors. The first is the number of photons absorbed and the second is the efficiency with which these absorbed photons lead to conduction band electrons. If we assume that the absorption probability is independent of cluster size, then the number of photons absorbed at each wavelength will depend only on the number of clusters absorbing at that wavelength. If there is a distribution of cluster sizes, with the smaller ones being in higher concentration, then the decrease in speed with increasing wavelength would be expected.

But, we also must include the effect of quantum yield of conduction band electrons. The quantum yield will be determined by the ability of the excited sensitizer center to inject a hole into the valence band before the electron returns to the ground state. The

quantum yield will then be determined by the ΔE_{act} for hole injection (Table 5). This activation energy will enter through the usual Boltzmann expression and will cause a rapid decrease in quantum yield with increasing wavelength. This will also cause a falloff in long wavelength speed.

In principle, we could assume a uniform distribution of cluster sizes and use the measured activation energies to calculate the relative speed at long wavelength. This could be compared to the measured wavelength dependence shown in Fig. 12 and 13. Any discrepancy with the experimental data could then be related to the distribution of number of sensitizer centers. Thus, we could derive the relative numbers of sensitizer centers at each wavelength. Unfortunately, the uncertainties in our activation energies are magnified by the Boltzmann expression so that no meaningful results can be obtained with the current data.

The lack of effect of sulfur level on the wavelength dependence (Fig.12) is also of interest. Higher sulfur levels merely produce a higher long wavelength speed. Evidently, whatever the cluster size distribution is at low levels of sulfur, it remains virtually the same at higher levels. Only the actual number of clusters increases with increasing sulfur level.

V. CONCLUSIONS

1. There is a significant increase in the long wavelength sensitivity for sulfur and sulfur-plus-gold sensitized AgBr emulsions when the coatings are given a 16-hour vacuum outgassing.

2. The temperature dependence of long wavelength sensitivity when corrected for that for blue exposures is a function of chemical sensitizer type and exposure wavelength. The sulfur sensitized emulsions show much more temperature dependence and less wavelength dependence than sulfur-plus-gold sensitized emulsions.

3. A proposed mechanism for environmental desensitization involves the injection of a hole from the ground state of the excited sensitizer center, resulting in an electron trapped at a sensitizer center. This trapped electron may then be thermally excited into the conduction band, recombine with a mobile hole, or be scavenged by a diffusing O_2 molecule which may serve as a recombination center for the mobile hole. The effect of vacuum outgassing on LIRF for different spectral regions of exposure supports this mechanism.

4. The activation energy which is obtained from the temperature dependence studies actually measures the thermal energy required to inject a hole into the valence band from the excited state of the sensitizer center and not for electron transfer from the sensitizer center to the conduction band as earlier work has claimed.

5. The thermal trap depth of electrons trapped at sensitizer centers is derived by correlating the environmental desensitization with the derived energy levels. The calculated thermal trap depth is a function of exposure wavelength, but not a function of sensitizer level. Since large uncertainties are involved in the thermal trap depth calculation, the thermal trap depths presented in this paper are only used to establish trends.

VI. REFERENCES

1. J. M. Harbison and H. E. Spencer, in The Theory of the Photographic Process, 4th ed., T. H. James, Ed., Macmillan, New York, 1977, p. 149.

2. N. F. Mott and R.W. Gurney, 2nd ed., University Press, Oxford, England,1948, p. 227-248.

3. J. W. Mitchell, *Rep. Prog. Phys.* **20**: 433 (1957).

4. R. K. Hailstone, Symposium on Electronic and Ionic Properties of Silver Halides, B. Levy, Ed., IS&T — The Society for Imaging Science and Technology, 1991, p. 102.

5. J. F. Hamilton, *Photogr. Sci. Eng.* **27**: 225 (1983).

6. J. F. Hamilton, J. M. Harbison, and D. L. Jeanmaire, *J. Imaging Sci.* **32**: 17 (1988).

7. L. Kellogg and J. Hodes, SPSE Conf. Rochester, 1987.

8. R. K. Hailstone, *Photogr. Sci. Eng.* **27**: 152 (1983).

9. T. H. James, in The Theory of the Photographic Process, 4th ed., T. H. James, Ed., Macmillan, New York, 1977, p. 161.

10. H. Hirsch, *J. Photogr. Sci.* **20**: 187 (1972).

11. R. K. Hailstone, *J. Photogr. Sci.* **32**: 25 (1984).

12. (a) T. H. James, *J. Photogr. Sci.* **20**: 182 (1972); (b) T. A. Babcock, W. C. Lewis, and T. H. James, *Photogr. Sci. Eng.* **15**: 297 (1971); (c) T. H. James, *Photogr. Sci. Eng.* **18**: 100 (1974).

13. J. F. Hamilton, *Photogr. Sci. Eng.* **13**: 331 (1969).

14. (a) John W. Moore and Ralph G. Pearson, in Kinetics and Mechanism, 3rd ed., p. 186; (b) Bjoern Reitstoeen and Vernon D. Parker, *J. Am. Chem. Soc.* **112:** 4968 (1990); (c) Yonghua Chen, Arvi Rauk, and E. Tschuikow-Roux, *J. Phys. Chem.* **95:** 9900 (1991).

15. W. West and P. B. Gilman, The Theory of the Photographic Process, 4th ed., T. H. James, Ed., Macmillan, New York, 1977, p. 251.
16. T. A. Babcock, W. C. Lewis, P. A. McCue, and T. H. James, *Photogr. Sci. Eng.* **16**: 104 (1972); T. Tani, *Photogr. Sci. Eng.* **28**: 150 (1984); A. A. Muenter, P. B. Gilman, J. R. Lenhard, and T. L. Penner, "Mechanistic Consequences of Anomously Efficient Spectral Sensitization by Desensitizing Dyes", The International East-West Symposium on the Factors Influencing Photographic Sensitivity, Oct/Nov 1984, Maui, Hawaii, paper C4.
17. C. R. Berry, *J. Photogr. Sci.* **18**: 169 (1970).
18. W. West and P. B. Gilman, in The Theory of the Photographic Process, 4th ed., T. H. James, Ed., Macmillan, New York, 1977, p. 252.
19. J. F. Hamilton, *J. Imaging Sci.* **34**: 1 (1990) and references cited therein.
20. T. H. James and W. Vanselow, *J. Phys. Chem.* **57**: 725 (1953); P. H. Roth and W. H. Simpson, *Photogr. Sci. Eng.* **24**: 133 (1980); D. J. Cash, *J. Photogr. Sci.* **29**: 133, 140 (1981)